STUDY OF PHASE TRANSITIONS AND CRITICAL POINTS IN THE RARE-EARTH REGION IN THE FRAMEWORK OF THE INTERACTING BOSON MODEL (IBM-1)

A Thesis

Submitted to the College of Science of
Al-Nahrain University in Partial Fulfillment of
the Requirements for the Degree of
Doctor of Philosophy in
Physics.

By

FOUAD ATTIA MAJEED AL-AJEELI

(*B.Sc. 1997*)

(*M.Sc. 1999*)

Sufar ***1426 H.***

April ***2005 A.D.***

بسم الله الرحمن الرحيم

﴿وَعِندَهُ مَفَاتِحُ الْغَيْبِ لَا يَعْلَمُهَا إِلَّا هُوَ وَيَعْلَمُ مَا فِي الْبَرِّ وَالْبَحْرِ وَمَا تَسْقُطُ مِن وَرَقَةٍ إِلَّا يَعْلَمُهَا وَلَا حَبَّةٍ فِي ظُلُمَاتِ الْأَرْضِ وَلَا رَطْبٍ وَلَا يَابِسٍ إِلَّا فِي كِتَابٍ مُّبِينٍ﴾

صدق الله العظيم

(من سورة الأنعام)

(الآية ٥٩)

Dedication

This thesis is dedicated to my parents

who gave me the tools to succeed

and

to brothers and sisters

who gave me the support to make it happen.

Supervisors Certificate

We certify that the thesis entitled "**Study of phase transitions and critical points in the rare-earth region in the frame work of the interacting boson model (IBM-1)**" was prepared by ***Mr. Fouad Attia Majeed*** under our supervision at ***Al-Nahrain University*** as partial fulfillment of the requirement for the degree of Doctor of Philosophy of Science in Theoretical Nuclear Physics.

Signature:
Name: Dr. Ra′ad A. Radhi
Title: Professor
(Supervisor)
Date: / /2005.

Signature:
Name: Dr. Siham A. Kandela
Title: Professor
(Supervisor)
Date: / /2005.

Signature:
Name: Dr. Saddon T. Ahmad
Title: Assistant Professor
(Supervisor)
Date: / /2005.

In view of the available recommendations, I forward this thesis for debate by the examining committee.

Signature:
Name: Dr. Ahmad K. Ahmad
Title: Assistant Professor
(Head of Physics Department)
Date: / /2005.

Committee Certificate

We Certify that we read this thesis entitled "***STUDY OF PHASE TRANSITIONS AND CRITICAL POINTS IN THE RARE-EARTH REGION IN THE FRAMEWORK OF THE INTERACTING BOSON MODEL (IBM-1)***" and as examining committee, examined the student ***FOUAD A. MAJEED*** in its context and in our opinion is adequate with ***EXCELLENT*** standing as thesis for the Degree of Doctor of Philosophy in Physics.

Signature:
Name: Dr. Khalid S. Ibrahim
Title: Professor
(Chairman)
Date: / /2005.

Signature:
Name: Dr. Mazin M. Elias
Title: Professor
(Member)
Date: / /2005.

Signature:
Name: Dr. Maher N. Sarsam
Title: Professor
(Member)
Date: / /2005.

Signature:
Name: Dr. Laith A. Al-Ani
Title: Assistant Professor
(Member)
Date: / /2005.

Signature:
Name: Dr. Jamal W. Salman
Title: Assistant Professor
(Member)
Date: / /2005.

Signature:
Name: Dr. Ra′ad A. Radhi
Title: Professor
(Member/Supervisor)
Date: / /2005.

Signature:
Name: Dr. Siham A. Kandela
Title: Professor
(Member/Supervisor)
Date: / /2005.

Signature:
Name: Dr. Saddon T. Ahmad
Title: Assistant Professor
(Member/Supervisor)
Date: / /2005.

Approved for **Al-Nahrain University,** College of Science.

Signature:
Name: Dr. Laith A. Al-Ani
Title: Assistant Professor
(Dean)
Date: / /2005.

Acknowledgments

Praise is to *Allah*, Mercy and peace are to the Prophet Mohammed and his relatives and companions.

First, I would like to thank my supervisors, Prof. Dr. Ra′ad A. Radhi, Prof. Dr. Siham A. Kandela and Dr. Saddon T. Ahmad for the countless hours that they dedicated to this thesis. Their understanding and expertise in my area of research greatly improved the contents of this thesis. I am grateful for their helpful comments, suggestions and constructive criticism throughout this project. My thesis has benefitted substantially from their insightful recommendations.

I would like to thank Prof. Francessco Iachello at Yale University for the time he spent answering my questions tirelessly. I am also extremely grateful to Prof. Piet Van Iscaker at GANIL/France, for his assistance in providing me with needed codes.

A word of thanks is due to staff members of the Physics Department in the College of Science at Al-Nahrain University for their help and kind assistance.

I wish to express my thanks to my friends, especially those in the dormitory, where I spent the most difficult and joyful times in my life.

I am grateful to my family for their constant love and support. Thanks for their understanding, never-ending encouragement, and support throughout this work.

Fouad

Abstract

A systematic study of isotope chains in the rare–earth region is presented. For the chains $^{144-154}_{60}\mathrm{Nd}$, $^{146-160}_{62}\mathrm{Sm}$, $^{148-162}_{64}\mathrm{Gd}$, *and* $^{150-166}_{66}\mathrm{Dy}$, *energy levels, E2 transition rates, and two–neutron separation energies* (S_{2n}) *are described by using the most general* (*up to two–body terms*) *IBM-1 Hamiltonian. For each isotope chain a general fit is performed in such a way that all parameters but one are kept fixed to describe the whole chain.*

In this region, nuclei evolve from spherical to deformed shapes and a method based on catastrophe theory, in combination with a coherent state analysis to generate the IBM-1 energy surfaces, is used to identify critical phase transition points.

The approach used to fix the Hamiltonian parameters leads to a very good global agreement with the recent available experimental data corresponding to excitation energies, B(E2)'s and S_{2n} *values. In particular, an excellent agreement with the measured* S_{2n} *values is obtained, which is considered a key observable to locate phase transitional regions. The analysis presented here is consistent with previous CQF studies in the same region. As a result we find that* ^{148}Nd *and* ^{150}Sm *are the best candidates to be critical, but we should remark that* ^{150}Nd *and* ^{152}Sm *are not far away from it.*

List of Contents

List of Figures

List of Tables

Chapter

1

Introduction

1.1 Geometric Symmetries

Symmetry is a unifying concept, introduced in physics in the second part of the 19th century, when it referred mainly to the geometric arrangement of constituent parts into the whole. An example is the arrangement of atoms in molecules and crystals (*point group symmetries*). At the beginning of the 20th century the concept was enlarged to include "*kinematical* (*or space-time*) *symmetries*", sometimes called "*fundamental*" symmetries. These symmetries are a generalization of the familiar translational and rotational invariance of non-relativistic systems to include time (Lorentz and Poincare' invariance). These symmetries are expected to be exact. To these symmetries parity, P, charge conjugation, C, and time reversal, T, invariance were later added. Although the product PCT is expected to be an exact symmetry (PCT theorem), the individual

parts may be broken [1].

1.2 Quantal Symmetries-Dynamical and Gauge

With the advent of quantum mechanics, the concept of symmetry was further enlarged. Two new types emerged: dynamic symmetries and gauge symmetries. Both are symmetries of the interactions, but dynamic symmetries govern the motion of particles in physical systems, while gauge symmetries relate to the fundamental interactions of Nature. Both of these symmetries have played a major role in the development of Physics in the 20^{th} century. It is now believed that all fundamental interactions are governed by gauge symmetries, $U(1)$ for electromagnetism, $SU(2)$ for weak interactions and $SU(3)$ for strong interactions [1].

1.3 Symmetries in Complex Systems

The symmetries of particular importance for complex systems, such as the atomic nucleus, are dynamic symmetries. The oldest example of this type of symmetry is that introduced in Atomic Physics by Wolfgang Pauli in 1926 (Dynamic symmetry of the Coulomb interaction). Murray Gell'Mann and Yuval Ne'eman introduced them in the 1960's in Particle Physics (Flavor symmetry). In 1974, they were introduced in Nuclear Physics (Interacting Boson Model) and in 1981 in Molecular Physics (Vibron Model) [2].

1.4 Dynamical Symmetries

In the last 30 years, several examples of dynamic symmetries have been discovered in nuclei. The quantum states of a physical system are characterized by a set of energy levels. Dynamic symmetries provide patterns of energy levels that can be easily recognized experimentally.

The patterns are characteristic of a certain group of transformations. For collective quadrupole motion $U(5)$, $SU(3)$ and $SO(6)$. All of these symmetries have been discovered and plotted in form of symmetry triangle known as "*Casten triangle*" as shown in Figure 1.1 [2].

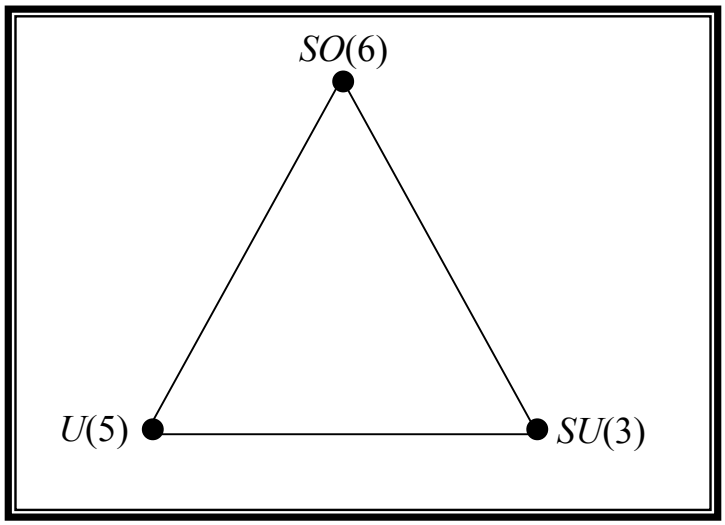

Figure 1.1: Symmetry triangle of the Interacting Boson Model (IBM-1) indicating the three limiting symmetries on each of the vertices and the transition legs between symmetries, taken from Ref. [2].

1.5 Dynamical Supersymmetries

The concept of symmetry was further enlarged in the 1970's to include symmetries involving simultaneously particles with integer and half integer spin (bosons and fermions). Such symmetries play a role in more than one area of physics. In particle physics, supersymmetries involving fundamental particles, quarks and squarks, photons and photinos, have been sought for decades but not yet found. Supersymmetries were introduced in nuclear physics in 1980 (Interacting Boson-Fermion Model). Contrary to the case of particle physics,

here the bosonic structures are composite entities, consisting of pairs of nucleons, similar to the Cooper pairs of the electron gas. Evidence for supersymmetry in nuclei was discovered in the 1980's and recently confirmed [2].

1.6 Critical Point Symmetries

Very recently, an astonishing result has been found, wherein systems at the critical point of quantum phase transitions (that is phase transitions that occur as a function of a coupling constant rather than the temperature) display a simple behavior. This simple behavior has been associated with the occurrence of a dynamical symmetry (meaning here solvability of the Hamiltonian problem). This suggestion, that appears to be experimentally verified in some nuclei, opens the way for a new area of symmetries studies, namely those of systems that are at the critical point of first and second order transitions [2].

In the last few years, interest for the study of phase transitions and phase coexistence in atomic nuclei has been revived [3, 4, 5, 6]. A new class of symmetries that applies to systems localized at the critical points has been proposed. In particular, the "*critical symmetry*" $E(5)$ [7] has been suggested to describe critical points in the phase transition from spherical to γ-unstable shapes while $X(5)$ is designed to describe systems lying at the critical point in the transition from spherical to axially deformed systems as shown in Figure 1.2 [8].

The Critical symmetries $X(5)$ and $E(5)$ are based originally on particular solutions of the Bohr-Mottelson differential equations, but are usually applied in the context of the Interacting Boson Model (IBM-1) [9], since the latter provides a simple but detailed framework in which first and second order phase transitions can be studied. In the IBM-1 language, the symmetry $E(5)$ corresponds to the critical point between the $U(5)$ and $O(6)$ symmetry limits, while the $X(5)$

symmetry should describe the phase transition region between the $U(5)$ and the $SU(3)$ dynamical symmetries, although the connection is not a rigorous one. Very recently the $O(6)$ limit itself has also been proposed to correspond to a critical point as shown in Figure 1.2 [10].

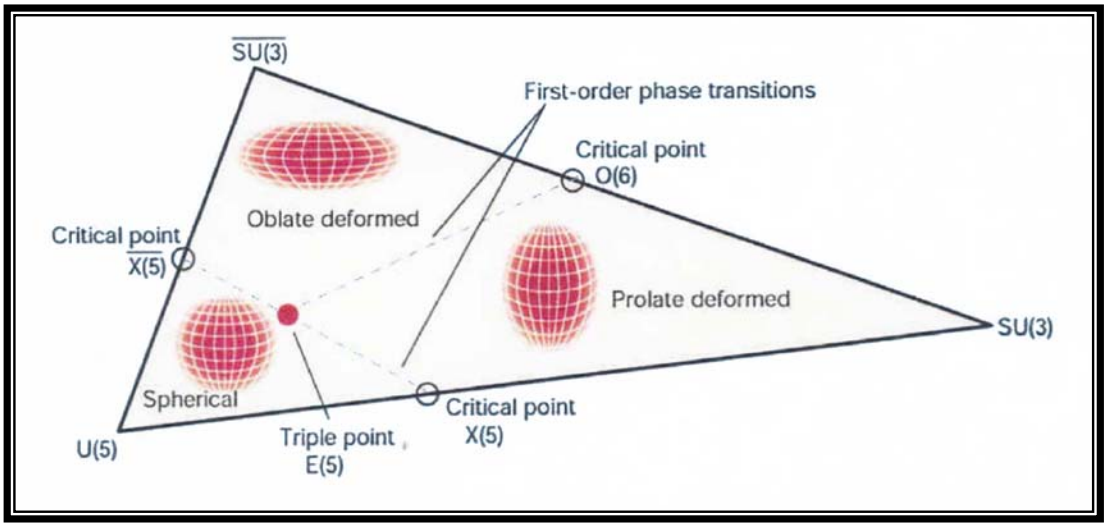

Figure 1.2: Phase diagram of the Interacting Boson Model (IBM-1) taken from Ref. [11].

Usually, the IBM-1 analyses of phase transitions have been carried out using schematic Hamiltonians in which the transition from one phase to the other is governed by a single parameter. It is thus necessary to see how much these predictions vary when a more general Hamiltonian is used.

The global approach was first used by Castaños *et al*. for the study of series of isotopes [12, 13, 14]. An alternative procedure is provided by the use of the Consistent Q Formalism (CQF) [15]. In this case, although the Hamiltonian is simpler than the general one, the main ingredients are included (the term concerning the $U(5)$ limit and Quadrupole –Quadrupole (Q-Q) interaction term concerning the $SU(3)$ limit). Within this scheme a whole isotope chain is described in terms of few parameters that change smoothly from one isotope to the next.

1.7 Literature Review

The first evidence for existence of critical point symmetries in nuclei were predicted by F. Iachello [7]. Iachello found analytic solutions at the critical point of such phase transitions: $E(5)$ for a transition between spherical and deformed γ-soft nuclei and $X(5)$ for a transition between spherical and axially deformed nuclei [8]. His approach is based on analytic solutions of Schrödinger equation corresponding to a geometric (Bohr) Hamiltonian with a square-well potential.

Extensive studies of R.F. Casten and R. Krücken *et al*. have shown that ^{152}Sm [16] and ^{150}Nd [17] are close manifestation of the $X(5)$ critical point model, by comparing the experimental data and their theoretical calculations of the ration of excitation energies, $R_{42} \equiv E(4_1^+)/E(2_1^+)$ and $R_{02} \equiv E(0_2^+)/E(2_1^+)$, also they compared their theoretical calculations for the transition probabilities $B(E2)$ with the measured transition probabilities.

J. Escher and A. Leviatan [18], presented the first example of a partial dynamical symmetry (PDS) in an interacting fermions system and demonstrated the close relationship of the associated hamiltonians with a realistic quadrupole-quadrupole interaction, thus shedding new light on this important interaction. Specifically, in the framework of the symplectic shell model of nuclei, they proved the existence of a family of fermionic Hamiltonians with partial $SU(3)$ symmetry. They briefly reviewed the symplectic theory, outlined the construction process for the PDS eigenstates with good symmetry and gave analytic expressions for the energies of these states and $E2$ transition strengths between them. Characteristics of both pure and mixed-symmetry PDS eigenstates are discussed and the resulting spectra and transition strengths are

compared to those of real nuclei. Their results showed that the PDS concept is relevant to the description of prolate, oblate, as well as triaxially deformed nuclei. They also considered similarities and differences between the fermion case and the previously established partial *SU*(3) symmetry in the Interacting Boson Model.

D. Bonatsos *et al.* [19], suggested a chain of potentials between the *U*(5) symmetry of the 5-dimensional harmonic oscillator and the *E*(5) symmetry, corresponding to U(5)↔O(6) phase transition. They predicted the Hamiltonian parameters independently for the spectra and *B*(*E2*) values. The ratio of excitation energies, $R_{42} \equiv E(4_1^+)/E(2_1^+)$ are derived numerically and compared with existing experimental data. In Addition they also suggested a chain potentials to the *U*(5) ↔*SU*(3) phase transition. They predicted the Hamiltonian parameters independently for the spectra and *B*(*E2*) values. The ratio of excitation energies, $R_{42} \equiv E(4_1^+)/E(2_1^+)$ are derived numerically and compared with existing experimental data.

V. Werner *et al*. [20], studied in terms of the Interacting Boson Model, the shape invariance for the ground state, formed by quadrupole moments up to sixth order, in the dynamical symmetry limits and over the whole structural range of the IBM-1.The results were related to the effective deformation parameters and their fluctuations in the geometrical model. They identified new signatures that can distinguish between vibrator and γ-soft rotor structures, and the one that is related to shape coexistence.

J. N.Ginocchio and A. Leviatan [21], studied the properties of critical points in the Interacting Boson Model (IBM-1), corresponding to flat-bottomed potentials as encountered in second-order phase transition between spherical and

deformed γ-unstable nuclei. They showed that the intrinsic states with an effective β-deformation reproduce the dynamics of the underlying non-rigid shapes. They concluded that the effective deformation could be determined from the global minimum of the energy surface after projection onto the appropriate symmetry and states of fixed number of bosons (N) and good $O(5)$ symmetry projected from these intrinsic states provided good analytic estimates to the exact eigenstates, energies and quadrupole transition rates at the critical point.

J. M. Arias *et al*. [22], investigated the quantum phase transition mechanisms that arise in the Interacting Boson Model (IBM-1). They showed that the second-order nature of the phase transition from $U(5)$ to $O(6)$ may be attributed to quantum integrability, whereas all the first-order phase transitions of the model are due to level with one singular point of level crossing. They proposed a model Hamiltonian with a true first-order phase transition for finite systems due to level crossing.

J. Dukelsky *et al*. [23], used the exact solution of the boson pairing Hamiltonian given by Richardson in the sixties to study the phenomena of level crossing and quantum phase transitions in the integrable regions of the *sd* and *sdg* interacting boson model.

J. P. Draayer *et al*. [24], used a mixed-symmetry nuclear shell-model scheme for carrying out calculations in regimes where there is a competition between two or more modes. A one dimensional toy model is used to demonstrate the concept. The theory is then applied to ^{24}Mg and ^{44}Ti. They also considered the $X(5)$ symmetry that falls along the $U(5)\leftrightarrow SU(3)$ leg of the interacting boson model. They concluded that the mixed-symmetry concept is effective, even when strong symmetry breaking occurs.

V. Werner *et al*. [25], discussed the concept of critical points in nuclear phase transitional regions from the standpoints of Q-invariants, simple observables and wave function entropy. They showed that these critical points are very closely coincide with the turning points of the discussed quantities, establishing the singular character of these points in nuclear phase transition regions between vibrational and rotational nuclei, with a finite number of particles.

E. A. McCutchan *et al*. [26], Populated excited, nonyrast states in ^{162}Yb via β^+/ε decay and studied through off-beam γ-ray spectroscopy at Yale University moving tape collector. New coincidence data provided evidence for a substational revision of the previous level scheme of ^{162}Yb is compared to the prediction of the *X*(5) critical point symmetry. They obtained good agreement for most energies while significant discrepancies exist with the current values of intraband *B*(*E*2) values.

R. Bijker *et al*. [27], presented the first extensive test of the critical point symmetry *X*(5) for the degree of freedom, based in part on recent measurements for the γ-band in ^{152}Sm. The agreement is good for some observable quantities including the energies and most intra- and inter-band transitions, but there is also a serious discrepancy for one transition.

Z. Jin-Fu *et al*. [28], analyzed the known low-lying levels and the E2 transition rates, they found that the empirical scheme of ^{114}Cd is in good overall agreement with the predictions of the transitional dynamical symmetry *E*(5) proposed by Iachello [8]. This suggests that ^{114}Cd may be better described by an *E*(5) nucleus than a *U*(5) nucleus as known before.

Z. Da-Li and L. Yu-Xin [29], analyzed the energy spectrum and $E2$ transition branching ratios, they show that the $E(5)$ symmetry predictions agree well with the experimental data of nucleus ^{130}Xe. Compared the calculated results with those within the framework of the interacting boson model, it is found that the nucleus ^{130}Xe is definitely a nucleus in the transitional region from $U(5)$ to $O(6)$ symmetry. The Nucleus ^{130}Xe is then another empirical evidence with $E(5)$ symmetry.

V. N. Zamfir and R. F. Casten [30], presented empirical realization of the $X(5)$ symmetry for recently studied phase transitional behavior in the evolution of nuclear structure from spherical to deformed shapes, their study has led to the development of a new class of symmetries, $E(5)$ and $X(5)$, describing analytically nuclei at the critical point of the phase transitions.

D. Tonev [31], measured the lifetime of states in ^{154}Gd by using the recoil distance Doppler-shift method following Coulomb excitation of ^{154}Gd by a 110 MeV ^{32}S beam. The experiment was performed at the University of Cologne. Reduced transition probabilities in ^{154}Gd are compared to the predictions of the critical point symmetry $X(5)$ of the phase/shape transition that occurs for the neutron number (N=90) rare earth isotones. Very good agreement was observed between the free parameter of $X(5)$ predictions and the low-spin level scheme of ^{154}Gd, revealing this nucleus as one of the best cases found thus far for the realization of the $X(5)$ symmetry.

In this work we follow references [12, 13, 14, 32, 33] and use a more general one–and two–body IBM-1 Hamiltonian to obtain the model parameters from a fit to energy levels of chains of isotopes. In this way a set of fixed parameters, with the exception of one that varies from isotope to isotope, is

obtained for each isotope chain and the transition phase can be studied in the general model space. The fit to a large data set in many nuclei diminishes the uncertainties in the parameter determination. A possible problem arising from working with such a general Hamiltonian is the difficulty in determining the position of the critical points. Fortunately, the methods of catastrophe theory [34] allow the definition of the essential parameters needed to classify the shape and stability of the energy surface [32, 33].

The aim of this research work is to study and analyze diverse spectroscopic properties of several isotope chains in the rare-earth region, in which shape transition from spherical to deformed shapes is observed. We combine this study with a coherent-state analysis and with catastrophe theory in order to localize the critical points and test the $X(5)$ predictions. In this proposal we show that the critical points can be clearly identified by means of a general theoretical approach.

1.8 Thesis Outline

The thesis is structured as follows: In chapter 2 we present the basic theory of the IBM-1 Hamiltonian used, the electromagnetic transition operators and the Hamiltonian for Consistent Q Formalism (CQF).

Global description of the least-square fit method made for the different isotope chains to obtain the best set of parameters Hamiltonian is presented in chapter 3.

Chapter 4 of this thesis is devoted to the description of the intrinsic state formalism that is used to generate the energy surfaces produced by the parameters obtained by the fit method presented in chapter 3, and how to identify

the location of the critical point in the shape transition for each isotope by using catastrophe theory, also in this chapter an alternative description provided by the CQF for the rare-earth region is briefly discussed.

Comparisons of the theoretical results with the experimental data for excitation energies, $E2$ transition rates and two-neutron separation energies are presented in Chapter 5. Also this chapter includes a comparison of experimental spectrum of ^{152}Sm with $X(5)$ model, our work and the work using CQF Hamiltonian. The discussion of these results with the conclusions and future work are presented in chapter 5.

Chapter

2

IBM-1 DESCRIPTION

2.1 Introduction

The Interacting Boson Model-1 (IBM-1) originated from early ideas of Feshbach and Iachello [9], who in 1969 described some properties of light nuclei in terms of interacting bosons, and from the work of Janssen *et al*. [35], who in 1974 suggested a description of collective quadrupole states in nuclei in terms of *SU*(6) group. The latter description was subsequently cast into a different mathematical form by Arima and Iachello [36] with the introduction of an s-boson, which made the *SU*(6), or rather *U*(6), structure more apparent. The success of this phonological approach to the structure of nuclei has led to major developments in understanding of nuclear structure.

The major new development was the realization that the bosons could be interpreted as nucleon pairs [37] in much the same way as Cooper pairs in the electron gas. This provided a framework for a microscopic description of collective quadrupole states in nuclei and stimulated a large number of theoretical investigations.

2.2 Boson Operators

In the interacting boson model, collective excitations of nuclei are described by bosons. An appropriate formalism to describe the situation is provided by second quantization. One thus introduces bosons creation (and annihilation) operators of multipolarity l and z-component m, $b^{\dagger}_{l,m}$ ($b_{l,m}$). A boson model is specified by number of boson operators that are introduced. In IBM-1, it is assumed that low-lying collective states of nuclei can be described in terms of a monopole bosons with angular momentum and parity $J^p = 0^+$, called s, and a quadrupole boson with $J^p = 2^+$, called d. Thus, the building blocks of this model are [9]:

$$\begin{cases} s^{\dagger}, d^{\dagger}_{\mu} & (\mu = 0, \pm 1, \pm 2), \\ s, d_{\mu} & (\mu = 0, \pm 1, \pm 2). \end{cases} \tag{2.1}$$

The operators in Eq. (2.1) satisfy Bose commutations relations:

$$\begin{aligned} &[s, s^{\dagger}] = 1; \qquad [s, s] = [s^{\dagger}, s^{\dagger}] = 0; \\ &[d_{\mu}, d^{\dagger}_{\mu'}] = \delta_{\mu\mu'}; \ [d_{\mu}, d_{\mu'}] = [d^{\dagger}_{\mu}, d^{\dagger}_{\mu'}] = 0; \\ &[s, d^{\dagger}_{\mu}] = [s, d_{\mu}] = [s^{\dagger}, d^{\dagger}_{\mu}] = [s^{\dagger}, d_{\mu}] = 0. \end{aligned} \tag{2.2}$$

The boson operators can be written in a more compact form as [9]:

$$b^{\dagger}_{l,m};\ b_{l,m};\qquad (l=0,2;\quad -l\le m\le l), \tag{2.3}$$

or

$$b^{\dagger}_{\alpha};\quad b_{\alpha};\qquad (\alpha=1,\ldots,6), \tag{2.4}$$

with

$$b_1=s,\qquad b_2=d_{+2},\qquad b_3=d_{+1},\qquad b_4=d_0,\quad b_5=d_{-1},\quad b_6=d_{-2} \tag{2.5}$$

The commutation relations Eq. (2.2) are written then as:

$$\begin{aligned}&[b_{l,m},b^{\dagger}_{l',m'}]=\delta_{ll'}\delta_{mm'};\\ &[b_{l,m},b_{l'm'}]=[b^{\dagger}_{l,m},b^{\dagger}_{l',m'}]=0,\end{aligned} \tag{2.6}$$

or as

$$[b_{\alpha},b^{\dagger}_{\alpha'}]=\delta_{\alpha\alpha'}\ ;\quad [b_{\alpha},b_{\alpha'}]=[b^{\dagger}_{\alpha},b^{\dagger}_{\alpha'}]=0. \tag{2.7}$$

For applications, one needs to construct with boson operators spherical tensors $T^{(k)}_{\kappa}$ of degree *k,* in the sense of Racah, i.e. operators that transform as basis vectors of a (2*k*+1) dimensional representation $R^{(k)}_{\kappa\kappa'}$ of the rotation group

$$\Re T^{(k)}_{\kappa}\Re^{-1}=\sum_{\kappa'}T^{(k)}_{\kappa'}R^{(k)}_{\kappa'\kappa} \tag{2.8}$$

The creation operators can be defined as Eq. (2.8). However, the annihilation operators

$$\widetilde{b}_{l,m}=(-1)^{l+m}b_{l,-m} \tag{2.9}$$

Eq. (2.9) gives, when applied to the present case,

$$\widetilde{s} = s, \quad \widetilde{d}_\mu = (-1)^\mu d_{-\mu} \tag{2.10}$$

With spherical tensors one can form tensor products. Using the notation of [38]:

$$T^{(k)}_\kappa = [T^{(k_1)} \times T^{(k_2)}]^{(k)}_\kappa \tag{2.11}$$

for the tensor product of $T^{(k_1)}$ and $T^{(k_2)}$, i.e. the square bracket indicates

$$[T^{(k_1)} \times T^{(k_2)}]^{(k)}_\kappa = \sum_{\kappa_1\kappa_2} (k_1\kappa_1 k_2\kappa_2 \mid k\kappa) T^{(k_1)}_{\kappa_1} T^{(k_2)}_{\kappa_2} \tag{2.12}$$

where the symbol $(k_1\kappa_1 k_2\kappa_2 \mid k\kappa)$ denotes a Clebsch-Gordon coefficient. A particular case of tensor product is the scalar product.

$$\left(U^{(k)} \cdot V^{(k)}\right) = (-1)^k (2k+1)^{\frac{1}{2}} [U^{(k)} \times V^{(k)}]^{(0)}_0 \tag{2.13}$$

This product can also be rewritten as

$$\left(U^{(k)} \cdot V^{(k)}\right) = \sum_\kappa (-1)^\kappa U^{(k)}_\kappa V^{(k)}_{-\kappa} \tag{2.14}$$

2.3 Basis States

Basis states can be constructed by repeated application of boson operators on a boson vacuum $|0\rangle$ [9],

$$\mathcal{B}: b^\dagger_\alpha b^\dagger_{\alpha'} \ldots |0\rangle. \tag{2.15}$$

It is convenient to construct states of good angular momentum by coupling the boson operators appropriately,

$$\mathcal{B}: [b^\dagger_l \times b^\dagger_{l'} \times \cdots]^{(L)}_M |0\rangle. \tag{2.16}$$

However, the total angular momentum alone is not, in general, sufficient to characterize the states uniquely, since there may be several states with the same L for a given number of bosons, N.

Most numerical calculations are performed by using so-called spherical basis in which the s and d bosons are explicitly separated.

$$\mathcal{B}^{(I)}\colon\ s^{\dagger n_s}[d^{\dagger n_d}]_{v n_\Delta L M_L}\left|0\right\rangle. \tag{2.17}$$

These are states with total boson number

$$N = n_s + n_d \tag{2.18}$$

where n_s and n_d are the numbers of s and d bosons. The numbers v, n_Δ are additional quantum numbers to identify all the possible resulted states.

2.4 The Lie Algebra *U*(6)

If we introduce the operators as in [39]:

$$G^k_\kappa(ll') = [b^\dagger_l \times \tilde{b}_{l'}]^{(k)}_\kappa \tag{2.19}$$

where $l, l' = 0, 2 \equiv s, d$. It so happens that the commutation relations of these operators equations among themselves are the same as the commutation relations of the Lie algebra of the group $U(6)$ of unitary transformation in 6 dimensions (Appendix B). These operators are thus identified as the generators of the algebra $U(6)$. Since they are the building blocks of the most general Hamiltonian one can write in the IBM-1 model, thus the Hamiltonian has the group structure of $U(6)$. There are in total $36=6^2$ of these generators, which can be written down explicitly as [39];

$$\left.\begin{aligned}
G_0^0(ss) &= [s^\dagger \times \tilde{s}]_0^{(0)}, \\
G_0^0(dd) &= [d^\dagger \times \tilde{d}]_0^{(0)}, \\
G_\kappa^1(dd) &= [d^\dagger \times \tilde{d}]_\kappa^{(1)}, \\
G_\kappa^2(dd) &= [d^\dagger \times \tilde{d}]_\kappa^{(2)}, \\
G_\kappa^3(dd) &= [d^\dagger \times \tilde{d}]_\kappa^{(3)}, \\
G_\kappa^4(dd) &= [d^\dagger \times \tilde{d}]_\kappa^{(4)}, \\
G_\kappa^2(ds) &= [d^\dagger \times \tilde{s}]_\kappa^{(2)}, \\
G_\kappa^2(sd) &= [s^\dagger \times \tilde{d}]_\kappa^{(2)}.
\end{aligned}\right\} \tag{2.20}$$

2.5 Casimir Operator

If G_κ^k be the generators of the Lie algebra G. One can identify some operators C, called **Casimir operators**, which have the property [39];

$$[C, G_\kappa^k] = 0 \quad \text{for any} \quad k, \kappa. \tag{2.21}$$

Thus by definition the Casimir operators of the group G commute with all generators of the group G, defined in Eq. (2.20). There exists at least one Casimir operator for each of the Lie algebras under study.

2.6 Physical Operators

2.6.1 The Hamiltonian operator

In order to calculate properties of physical system described by the bosons, one can write all operators in terms of boson operators. If the number of bosons N is conserved, the Hamiltonian operator of the system can be written as [9]:

$$H = E_0 + \sum_{\alpha\beta} \varepsilon_{\alpha\beta} b_\alpha^\dagger b_\beta + \sum_{\alpha\beta\gamma\delta} \tfrac{1}{2} u_{\alpha\beta\gamma\delta} b_\alpha^\dagger b_\beta^\dagger b_\gamma b_\delta + \cdots. \tag{2.22}$$

Here E_0 is a constant number, the second term with $b^\dagger b$ represents one-body contributions, the next one represents two-body contributions, etc. The

presence of the interaction terms gives the name 'Interacting boson models' to this type of models.

In most calculations, only up to two-body terms have been retained. When written explicitly in terms of s and d bosons as:

$$\begin{aligned} H = {} & E_0 + \varepsilon_s (s^\dagger \cdot \tilde{s}) + \varepsilon_d (d^\dagger \times \tilde{d}) \\ & + \sum_{L=0,2,4} \tfrac{1}{2}(2L+1)^{\frac{1}{2}} c_L [[d^\dagger \times d^\dagger]^{(L)} \times [\tilde{d} \times \tilde{d}]^{(L)}]_0^{(0)} \\ & + \frac{1}{\sqrt{2}} v_2 [[d^\dagger \times d^\dagger]^{(2)} \times [\tilde{d} \times \tilde{s}]^{(2)} + [d^\dagger \times s^\dagger]^{(2)} \times [\tilde{d} \times \tilde{d}]^{(2)}]_0^{(0)} \\ & + \tfrac{1}{2} v_0 [[d^\dagger \times d^\dagger]^{(0)} \times [\tilde{s} \times \tilde{s}]^{(0)} + [s^\dagger \times s^\dagger]^{(0)} \times [\tilde{d} \times \tilde{d}]^{(0)}]_0^{(0)} \\ & + u_2 [[d^\dagger \times s^\dagger]^{(2)} \times [\tilde{d} \times \tilde{s}]^{(2)}]_0^{(0)} + \tfrac{1}{2} u_0 [[s^\dagger \times s^\dagger]^{(0)} \times [\tilde{s} \times \tilde{s}]^{(0)}]_0^{(0)}. \end{aligned} \tag{2.23}$$

The Hamiltonian operator in Eq. (2.23) is a Hermitian operator, i.e. $H^\dagger = H$. Thus, there are two one-body terms, specified by the parameters $\varepsilon_s, \varepsilon_d$, and seven two-body terms, specified by the parameters c_L (L=0, 2, 4), v_L (L=0, 2), u_L (L=0, 2), to this order.

The general IBM-1 Hamiltonian can be expressed as [9];

$$\begin{aligned} H = {} & E_0 + \alpha_1 C_1[U(5)] + \alpha_2 C_2[U(5)] + \alpha_3 C_2[SO(5)] \\ & + \alpha_4 C_2[SO(3)] + \alpha_5 C_2[SO(6)] + \alpha_6 C_2[SU(3)] \end{aligned} \tag{2.24}$$

where $\alpha_1, \alpha_2, \alpha_3, \alpha_4, \alpha_5$ and α_6 are six independent free parameters, which are fitted to experimental data, C_1 and C_2 stand for the first and the second rank Casimir invariants of the algebras entering the reduction chains of the U(6) algebra [39]:

$$\left.\begin{array}{ll} U(6) \supset U(5) \supset SO(5) \supset SO(3) \supset SO(2) & I \\ U(6) \supset U(3) \supset SU(3) \supset SO(3) \supset SO(2) & II \\ U(6) \supset SO(6) \supset SO(5) \supset SO(3) \supset SO(2) & III \end{array}\right\} \tag{2.25}$$

The generators of algebras $U(6)$, $U(5)$, $SU(3)$, $SO(6)$, $SO(5)$ and $SO(3)$, can be written in multipolar form operators as in Table (2-1) [31];

Table (2-1): Generators of $U(6)$, $U(5)$, $SU(3)$, $SO(6)$, $SO(5)$ and $SO(3)$ algebras

Algebra	Generators
$U(6)$	$[d^\dagger \times s]^{(2)}_\kappa$, $[s^\dagger \times \tilde{d}]^{(2)}_\kappa$, $\hat{S} = [s^\dagger \times s]^{(0)}_0$, $\hat{T}^{(k)}_\kappa = [d^\dagger \times \tilde{d}]^{(k)}_\kappa$, k=0,1,2, 3, 4
$U(5)$	$\hat{T}^{(k)}_\kappa = [d^\dagger \times \tilde{d}]^{(k)}_\kappa$, k=0,1,2, 3, 4
$SU(3)$	$\hat{Q}_\kappa = [d^\dagger \times s + s^\dagger \times \tilde{d}]^{(2)}_\kappa - \frac{\sqrt{7}}{2}[d^\dagger \times \tilde{d}]^{(2)}_\kappa$, $\hat{L}_\kappa = [d^\dagger \times \tilde{d}]^{(1)}_\kappa$
$SO(6)$	$Q^0_\kappa = [d^\dagger \times s + s^\dagger \times \tilde{d}]^{(2)}_\kappa$, $\hat{T}^{(k)}_\kappa = [d^\dagger \times \tilde{d}]^{(k)}_\kappa$, k=1, 3
$SO(5)$	$\hat{T}^{(k)}_\kappa = [d^\dagger \times \tilde{d}]^{(k)}_\kappa$, k=1, 3
$SO(3)$	$\hat{L}_\kappa = [d^\dagger \times \tilde{d}]^{(1)}_\kappa$

The Casimir operators can be written in terms of the generators of the reduction chains of the $U(6)$ algebra as [9]:

$$\left.\begin{aligned} &C_1[U(5)] = \hat{n}_d, && C_2[SO(5)] = 2(\hat{T}^{(3)} \cdot \hat{T}^{(3)}) + 2(\hat{T}^{(1)} \cdot \hat{T}^{(1)}), \\ &C_2[U(5)] = \hat{n}_d(\hat{n}_d + 4), && C_2[SO(6)] = \hat{N}(\hat{N} + 4) - 4(\hat{P}^\dagger \cdot \hat{P}), \\ &C_2[SO(3)] = 10(\hat{T}^{(1)} \cdot \hat{T}^{(1)}), && C_2[SU(3)] = 2(\hat{Q} \cdot \hat{Q}) + \tfrac{15}{2}(\hat{T}^{(1)} \cdot \hat{T}^{(1)}). \end{aligned}\right\} \quad (2.26)$$

where generators of the groups entering reduction chains Eq. (2.25) are given in Table (2-1), and

$$\left.\begin{aligned} &\hat{n}_d = (d^\dagger \cdot \tilde{d}), \\ &\hat{P} = \left((\tilde{d} \cdot \tilde{d}) - (s \cdot s)\right), \\ &\hat{L} = \sqrt{10}(d^\dagger \cdot \tilde{d})^{(1)}, \\ &E_0 = \tilde{A}\hat{N} + \tilde{B}\frac{\hat{N}(\hat{N}-1)}{2} \end{aligned}\right\} \quad (2.27)$$

Combining equations (2.24), (2.26) and (2.27), the most general (including up to two–body terms) IBM-1 Hamiltonian, can be written as [9]:

$$\hat{H} = \widetilde{A}\hat{N} + \widetilde{B}\frac{\hat{N}(\hat{N}-1)}{2} + \varepsilon_d \hat{n}_d + k_0 \hat{P}^\dagger \hat{P} + k_1 \hat{L}\cdot\hat{L} + k_2 \hat{Q}\cdot\hat{Q} + k_3 \hat{T}_3 \cdot \hat{T}_3 + k_4 \hat{T}_4 \cdot \hat{T}_4 \tag{2.28}$$

where $\hat{N}$, and $\hat{n}_d$ are the total boson number operator, and the *d* boson number operator, respectively. The six independent free parameters $\varepsilon_d, k_0, k_1, k_2, k_3,$ and k_4 to be determined by using the least square fit method to experimental data.

The first two terms in the Hamiltonian do not affect the spectra but only the binding energy. Therefore, they can be removed from the Hamiltonian if only the excitation spectrum of the system is of interest. However, a complete description of both excitation and binding energies requires the use of the full Hamiltonian Eq. (2.28).

2.6.2 Transition operators

Operators inducing electromagnetic transitions of multipolarity *L* can also be written in terms of boson operators as [9]:

$$T^{(L)} = t_0^{(0)}\delta_{L0} + \sum_{\alpha\beta} t_{\alpha\beta}^{(L)} b_\alpha^\dagger b_\beta + \cdots \tag{2.29}$$

Again, since the operators must transform as tensors of rank *L* under rotations, it is more convenient to introduce coupled tensors as

$$T_\mu^{(L)} = t_0^{(0)}\delta_{L0} + \sum_{ll'} t_{ll'}^{(L)} [b_l^\dagger \times \widetilde{b}_{l'}]_\mu^{(L)} + \cdots. \tag{2.30}$$

Usually, one stops at one body terms. One can again write down explicitly the operators Eq. (2.30) in terms of s and d bosons as [9]:

$$\left.\begin{aligned} T_0^{(\mathrm{E0})} &= \gamma_0 + \alpha_0[s^\dagger \times \tilde{s}]_0^{(0)} + \beta_0[d^\dagger \times \tilde{d}]_0^{(0)}, \\ T_\mu^{(\mathrm{M1})} &= \beta_1[d^\dagger \times \tilde{d}]_\mu^{(1)}, \\ T_\mu^{\mathrm{E2}} &= \alpha_2[s^\dagger \times \tilde{d} + d^\dagger \times \tilde{s}]_\mu^{(2)} + \beta_2[d^\dagger \times \tilde{d}]_\mu^{(2)}, \\ T_\mu^{(\mathrm{M3})} &= \beta_3[d^\dagger \times \tilde{d}]_\mu^{(3)}, \\ T_\mu^{(\mathrm{E4})} &= \beta_4[d^\dagger \times \tilde{d}]_\mu^{(4)} \end{aligned}\right\} \quad (2.31)$$

In this work we will focus on *E*2 transitions. The most general *E*2 transition operator including up to one-body terms can be written as [7]:

$$\hat{T}_M^{E2} = e_{eff}\left[\left(s^\dagger \times \tilde{d} + d^\dagger \times \tilde{s}\right)_M^{(2)} + \chi\left(d^\dagger \times \tilde{d}\right)_M^{(2)} \right] \quad (2.32)$$

where e_{eff} is the boson effective charge measured in units ($e.b$) and χ is a structure parameter.

2.7 Neutron separation energies

Two-neutron separation energies (S_{2n}) studied in the present work defined as the difference in binding energy between an even-even isotope and the preceding even-even one [40]:

$$S_{2n} = BE(N) - BE(N-1) \quad (2.33)$$

where N corresponds to the total number of bosons. Note that if only the first two terms in equation (2.28) are considered and $\tilde{A}$ and $\tilde{B}$ are assumed to be constant along the isotope chain, S_{2n} would be given by [40]:

$$S_{2n} = -\left(\tilde{A} - \frac{1}{2}\tilde{B}\right) - \tilde{B}N = A + BN \quad (2.34)$$

2.8 The CQF Hamiltonian

An alternative approach to describe long chains of rare-earth nuclei is to use the CQF. The CQF Hamiltonian is given as [41]:

$$\hat{H} = \varepsilon\, \hat{n}_d + k\hat{Q}' \cdot \hat{Q}' \tag{2.35}$$

with

$$\hat{Q}' = \left(s^{\dagger} \times \tilde{d} + d^{\dagger} \times \tilde{s}\right)^{(2)} + \chi\left(d^{\dagger} \times \tilde{d}\right)^{(2)} \tag{2.36}$$

For each nucleus the parameters ε, k and χ are determined in order to fit the excitation energies and $B(E2)$'s. In particular in Ref. [42] the parameters of the Hamiltonian are calculated within the CQF framework where the strength of the quadrupole term (Q-Q interaction term concerning the $SU(3)$ limit) of the Hamiltonian remains constant along a wide region of the mass table. As in the present thesis they compare experimental data and theoretical values for excitation energies and $B(E2)$ transition rates.

After getting the best set of parameters from the least square fit method, the Hamiltonian equation (2.28) is calculated by the modified version of the computer code PHINT originally written by O. Scholten [43] with technical notes (Appendix A) which is called (PCIBAXW) [44], where the boson energy matrix element are constructed using Fractional Parentage Coefficient (FPC) is diagonalized to get the excitation energy for each isotope in each isotopic chain, while the probability of transition $B(E2)$ values are calculated using the computer code (PCIBAEM) [45].

Chapter 3

Least-Squares Fitting Method

3.1 Selection of Experimental Data

Several isotope chains belonging to the rare-earth region were analyzed using the most general IBM-1 Hamiltonian, Eq. (2.28), and *E*2 transition operator, Eq. (2.32). For each chain of isotopes we will assume a single Hamiltonian, and a single *E*2 transition operator. All parameters in these operators are kept fixed for a given isotope chain, except for the single particle energy which is allowed to vary slightly from isotope to isotope. The way of fixing the best set of parameters in the Hamiltonian is to carry out a least-square fit procedure of the excitation energies of selected states (2_1^+, 4_1^+, 6_1^+, 8_1^+, 0_2^+, 2_3^+, 4_3^+, 2_2^+, 3_1^+, and 4_2^+) and the two neutron separation energies of all isotopes

in each isotopic chain. Once the parameters in the Hamiltonian are obtained, the $B(E2)$ transition probabilities $2_1^+ \to 0_1^+$, $4_1^+ \to 2_1^+$, $2_2^+ \to 0_1^+$, $2_3^+ \to 0_1^+$, and $0_3^+ \to 2_1^+$ of the set of isotopes are used to fix e_{eff} and χ by carrying out a least-square fit. The experimental data for excitation and binding energies and $B(E2)$'s have been taken from references [46, 47, 48, 49, 50, 51, 52, 53, 54, 55, 56, 57]. Finally, following Ref. [40] the Hamiltonian parameters were fixed just using the data for excitation energies and then A and B were adjusted to reproduce the experimental values of S_{2n}.

3.2 Determination of Parameters

The general procedure of each step will be outlined below, is illustrated schematically in Figure 3.1. First the eigenvalues of the Hamiltonian are expressed linearly in terms of the parameters appeared in Eq. (2.28). This can be done once the Hamiltonian matrix H is diagonalized for initial set of (guessed) parameters. The eigenvalues obtained from the initial set of parameters will, in general, not yield the optimum agreement with the experimental data. The set of parameters can be improved in a second step from least-square fit to the data that is wanted. With the new set of parameters, one can constructs and diagonalizes the Hamiltonian again [58].

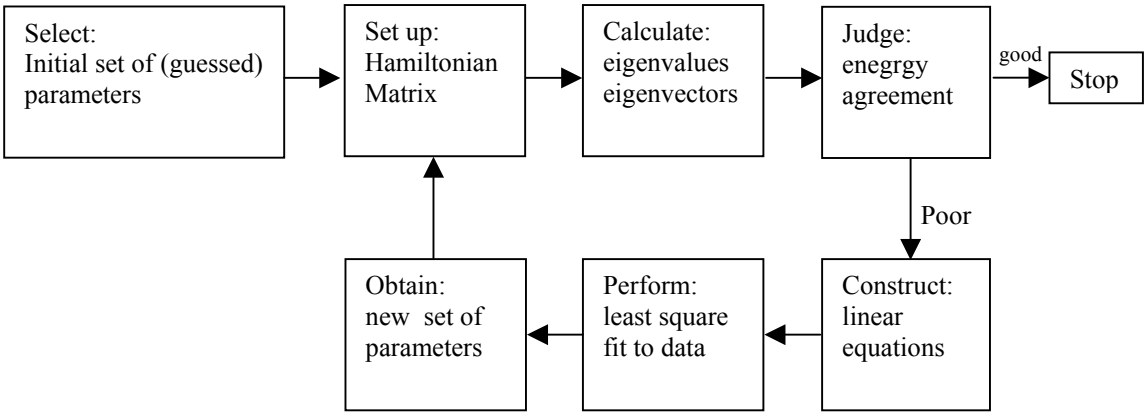

Figure 3.1: Schematic illustration of the various steps necessary to obtain the best set of parameters from a fit to experimental energies.

3.2.1 Construction of linear equations

The determination of the single-particle energies and two-body matrix elements from a comparison between calculated and experimentally determined energy levels is not a linear problem. The energy levels are obtained as the eigenvalues of the Hamiltonian matrices.

The energies of a nuclear system are determined by solving the eigenvalue problem for the Hamiltonian [58]:

$$H\Psi = E\Psi \tag{3.1}$$

Each eigenvector $\Psi_p (p = 1,\ldots,n)$, belonging to eigenvalue E_p, can be expanded in terms of the basis states Φ_k as

$$\Psi_p = a_{1p}\Phi_1 + a_{2p}\Phi_2 + \ldots + a_{np}\Phi_n \tag{3.2}$$

The Shrödinger equation (3.1) can now be rewritten in matrix form as

$$\begin{pmatrix} H_{11} \ldots H_{1n} \\ \vdots \quad\quad \vdots \\ H_{n1} \ldots H_{nm} \end{pmatrix} \begin{pmatrix} a_{1p} \\ \vdots \\ a_{np} \end{pmatrix} = E_p \begin{pmatrix} a_{1p} \\ \vdots \\ a_{np} \end{pmatrix} \qquad \text{for } p=1, 2,\ldots,n. \tag{3.3}$$

The matrix elements $H_{kl} = H_{lk}$ can be written for the n eigenvalue equations (3.3) can be represented by one matrix equation as

$$A^{-1}HA = A^T HA = \begin{pmatrix} a_{11} \ldots a_{n1} \\ \vdots \quad\quad \vdots \\ a_{1p} \quad a_{np} \\ \vdots \quad\quad \vdots \\ a_{1n} \quad a_{nn} \end{pmatrix} \begin{pmatrix} H_{11} \ldots H_{1n} \\ \\ \vdots \quad\quad\quad \vdots \\ \\ H_{n1} \ldots H_{nn} \end{pmatrix} \begin{pmatrix} a_{11} \ldots a_{1p} \ldots a_{1n} \\ \\ \vdots \quad\quad\quad\quad \vdots \\ \\ a_{n1} \ldots a_{np} \ldots a_{nn} \end{pmatrix} = \begin{pmatrix} E_1 & & & & 0 \\ & \ddots & & & \\ & & E_p & & \\ & & & \ddots & \\ 0 & & & & E_n \end{pmatrix} \tag{3.4}$$

Here the orthogonal matrix A is obtained by juxtaposition of the n column vectors $a_{kp}(k=1,2,\ldots,n)$. Since the matrix A is orthogonal, the inverse and transpose are equal, $A^{-1}=A^{T}$. Eq (3.4) reads with the summations in explicit form,

$$\left\langle A^{-1}HA\right\rangle_{p'p}=\sum_{j=1}^{n}\sum_{i=1}^{n}a_{jp'}H_{ji}a_{ip}=E_{p}\delta_{p'p}\quad\text{for }p',p=1,\ldots,n \tag{3.5}$$

This equation is equivalent to the relation

$$\left\langle\Psi_{p'}\middle|H\middle|\Psi_{p}\right\rangle=E_{p}\delta_{p'p}\qquad\text{for }\ p',p=1,\ldots,n. \tag{3.6}$$

Since each matrix element H_{ji} of the Hamiltonian is a linear combination of the single-particle energies and/or two-body matrix elements, we can write

$$H_{ji}=H_{ij}=\sum_{r=1}^{N_x}c_{r}^{(ij)}x_{r}, \tag{3.7}$$

where N_x gives the total number of parameters x_r and the geometrical coefficients $c_r^{(ij)}$ derive from Racah algebra. Substitution of Eq. (3.7) into Eq. (3.5) yields

$$\sum_{j=1}^{n}a_{jp}\sum_{i=1}^{n}(\sum_{r=1}^{N_x}c_{r}^{(ij)}x_{r})a_{ip}=E_{p}. \tag{3.8}$$

A rearrangement of the coefficients then leads to a set of simultaneous linear equations in the parameters x_r given by

$$\sum_{r=1}^{N_x}b_{r}^{(p)}x_{r}=E_{p}\qquad\text{for }p=1,\ldots,n. \tag{3.9}$$

with

$$b_r^{(p)} = \sum_{j=1}^{n} a_{jp} \sum_{i=1}^{n} a_{ip} c_r^{(ij)} \tag{3.10}$$

Thus, the Hamiltonian can be evaluated for some initial "best-guess" set of parameters and subsequently be diagonalized. This diagonalization leads to a matrix a_{ij} . Then Eq. (3.10) will provide us with an initial set of coefficients $b_r^{(p)}$ to be used in Eq. (3.9). Substitution of the "*best-guess*" set of parameters into Eq. (3.9) leads to same eigenvalues E_p that were obtained already from the diagonalization of the Hamiltonian.

Now if we replace the right-hand side of Eq. (3.9) by the corresponding experimental energies $E_{\text{exp}}^{(p)}$ and consider the x_r as unknown parameters. This leads to a set of equations

$$\sum_{r=1}^{N_x} b_r^{(p)} x_r = E_{\text{exp}}^{(p)} \qquad \text{with } p=1,\ldots,n. \tag{3.11}$$

where the coefficients $b_r^{(p)}$ are defined in Eq. (3.10). It is not necessary to consider only one nucleus at a time for the fitting procedure. Usually one takes into account many levels of different spin J in several neighboring nuclei simultaneously. The total number of parameters N_x then remains the same of course, but the number of equations to be satisfied increases appreciably. Therefore, the index p (labelling states of one matrix) by the index q, which labels the complete set of equations that result from all matrices taken together

$$\sum_{r=1}^{N_x} b_r^{(q)} x_r = E_{\text{exp}}^{(q)} \qquad \text{with } q=1,\ldots,N_q \tag{3.12}$$

In order to obtain meaningful solution of this set of N_q equations in N_x

parameters with least square fitting procedure, the condition $N_q > N_x$ must be satisfied.

So far we have restricted ourselves to the determination of the interaction parameters with Eq. (3.12), where the values $E_{\text{exp}}^{(q)}$ denote the Coulomb-corrected binding energies of the states labeled q. Since the Coulomb contribution is usually assumed to be equal for ground-state and excited-state binding energies of one nucleus, it has no effect on differences of binding energies. Thus, knowledge of the Coulomb contribution is in general not necessary when only experimental excitation energies instead of binding energies are used in the fit. Thus, the parameters from the set of equations can be determined.

$$\sum_{r=1}^{N_x} (b_r^{(q)} - b_r^{(q_0)}) x_r = E_{\text{exp}}^{(q)} - E_{\text{exp}}^{(q_0)} \tag{3.13}$$

where the coefficients $b_r^{(q)}$ refer to excited states and the coefficients $b_r^{(q_0)}$ to the corresponding ground states.

3.2.2 The least-square fitting procedure

The set of constructed linear equations can be expressed as [58]:

$$\begin{array}{cccc} b_1^{(1)} x_1 & + b_2^{(1)} x_2 & + \ldots + b_{N_x}^{(1)} x_{N_x} & = E_{\text{exp}}^{(1)} \\ \vdots & \vdots & \vdots & \vdots \\ b_1^{(N_q)} x_1 & + b_2^{(N_q)} x_2 & + \ldots + b_{N_x}^{(N_q)} x_{N_x} & = E_{\text{exp}}^{(N_q)} \end{array} \tag{3.14}$$

the parameters x_r determined with the condition that the left-hand side approximates the experimental energies as closely as possible.

In least square method one minimizes the function:

$$Q^2 = \sum_{q=1}^{N_q} \left(\sum_{i=1}^{N_x} b_i^{(q)} x_i - E_{\exp}^{(q)} \right)^2 \tag{3.15}$$

since the experimental energies are uncorrelated, thus by varying parameters x_i until the minimum value of Q^2 is reached when the partial derivatives satisfy the relations:

$$\frac{\partial Q^2}{\partial x_r} = 0 \qquad \text{for} \qquad r = 1, \cdots, N_x. \tag{3.16}$$

Insertion Eq. (3.2) into Eq. (3.3) leads to:

$$\frac{\partial Q^2}{\partial x_r} = \sum_{q=1}^{N_q} \left(\sum_{i=1}^{N_x} b_i^{(q)} x_i - E_{\exp}^{(q)} \right) b_r^{(q)} = 0 \qquad \text{for } r = 1, \cdots, N_x, \tag{3.17}$$

or

$$\sum_{i=1}^{N_x} \sum_{q=1}^{N_q} b_r^{(q)} b_i^{(q)} x_i = \sum_{q=1}^{N_q} b_r^{(q)} E_{\exp}^{(q)} \qquad \text{with} \quad r = 1, \cdots, N_x. \tag{3.18}$$

The set of N_x linear equations in the N_x parameters can be written into matrix notation as follows:

$$\begin{pmatrix} b_1^{(1)} & \cdots & b_1^{(N_q)} \\ \vdots & & \vdots \\ b_{N_x}^{(1)} & \cdots & b_{N_x}^{(N_q)} \end{pmatrix} \begin{pmatrix} b_1^{(1)} & \cdots & b_{N_x}^{(1)} \\ \vdots & & \vdots \\ b_1^{(N_q)} & \cdots & b_{N_x}^{(N_q)} \end{pmatrix} \begin{pmatrix} x_1 \\ \vdots \\ x_{N_x} \end{pmatrix} = \begin{pmatrix} b_1^{(1)} & \cdots & b_1^{(N_q)} \\ \vdots & & \vdots \\ b_{N_x}^{(1)} & \cdots & b_{N_x}^{(N_q)} \end{pmatrix} \begin{pmatrix} E_{\exp}^{(1)} \\ \vdots \\ E_{\exp}^{(N_q)} \end{pmatrix} \tag{3.19}$$

or

$$B^T B X = B^T E_{\exp} \tag{3.20}$$

finally the resulted linear non-homogenous equations for the N_x parameters $x_1, x_2, \cdots, x_{N_x}$ can be solved with standard procedures leading to a new set of parameters $x_r^{(1)}$.

3.2.3 The iteration procedure

As the set of parameters $x_r^{(1)}$ improved one recalculates the matrix elements of the Hamiltonian. After diagonalization a new set of eigenvectors a_{kq} is obtained. From these one constructs set of equations (3.12) with coefficients $b_r^{(q)}$.

After least-squares fitting this leads to a second set of parameters $x_r^{(2)}$. This procedure must be repeated until convergence is obtained, i.e. until $x_r^{(n)} \approx x_r^{(n-1)}$. It is found that the number of iteration needed is of the order of the times smaller than the number of equations N_q. For $N_q >> N_x$ a faster convergence can be expected.

The best set of parameters can be reached as the root mean square (RMS) deviation made minimum. The RMS deviation is defined as [58]:

$$\Delta_{RMS} = \sqrt{\sum_{i=1}^{N_q} \left(E_{calc}^{(i)} - E_{\exp}^{(i)}\right)^2 / \left(N_q - N_x\right)} \qquad (3.21)$$

Chapter 4

ENERGY SURFACES AND PHASE TRANSITIONS

4.1 Intrinsic-State Formalism

The study of phase transitions in the IBM-1 requires the use of the so-called intrinsic-state formalism [59, 60, 61], although other approaches can be used [5, 62]. This formalism is very useful to discuss phase transitions in finite systems such nuclei and atoms because it provides a description of the behavior of a macroscopic system up to $1/N$ effects. To define the intrinsic, or coherent state, it is assumed that the dynamical behavior of the system can be described in terms of independent bosons "*dressed bosons*" moving in an average field [63].

The ground state of the system is a condensate, $|c\rangle$ of bosons occupying the lowest–energy phonon state, $\Gamma_c^\dagger$,

$$|c\rangle = \frac{1}{\sqrt{N!}}\left(\Gamma_c^\dagger\right)^N|0\rangle \tag{4.1}$$

where

$$\Gamma_c^\dagger = \frac{1}{\sqrt{1+\beta^2}}\left(s^\dagger + \beta\cos\gamma\, d_0^\dagger + \frac{1}{\sqrt{2}}\beta\sin\gamma\left(d_2^\dagger + d_{-2}^\dagger\right)\right) \tag{4.2}$$

and β and γ are variational parameters related with the shape variables in the geometrical collective model. The expectation value of the Hamiltonian in the intrinsic state Eq. (4.1) provides the energy surface of the system, $E(N,\beta,\gamma) = \langle c|\hat{H}|c\rangle$. The energy surface in terms of the parameters of the Hamiltonian Eq. (2.28) and the shape variables can be readily obtained [64],

$$\begin{aligned}\langle c|\hat{H}|c\rangle = {} & \frac{N\beta^2}{(1+\beta^2)}\left(\varepsilon_d + 6k_1 - \frac{9}{4}k_2 + \frac{7}{5}k_3 + \frac{9}{5}k_4\right) \\ & + \frac{N(N-1)}{(1+\beta^2)^2}\left[\frac{k_0}{4} + \beta^2\left(-\frac{k_0}{2} + 4k_2\right) + 2\sqrt{2}\beta^3 k_2\cos(3\gamma)\right. \\ & \left. + \beta^4\left(\frac{k_0}{4} + \frac{k_2}{2} + \frac{18}{35}k_4\right)\right]\end{aligned} \tag{4.3}$$

where the terms which do not depend on β and/or γ (corresponding to $\widetilde{A}$ and $\widetilde{B}$ in Eq. (2.28) have not been included.

The equilibrium values of the variational parameters β and γ are obtained by minimization of the ground state energy $\langle c|\hat{H}|c\rangle$. As mentioned above these parameters are related to the parameters of the Geometrical Collective Model and provide an image of the nuclear shape for a given IBM-1 Hamiltonian.

A spherical nucleus has a minimum in the energy surface at $\beta = 0$, while for a deformed one the energy surface has a minimum at a finite value of β and $\gamma = 0$ (prolate nucleus) or $\gamma = \pi/3$ (oblate nucleus). Finally, a γ-unstable nucleus corresponds to the case in which the energy surface has a minimum at a particular value of β and is independent of the value of γ. The equilibrium values of β and γ are the order parameters to study the phase transition of the system, although in the case under consideration (IBM-1) only β has to be taken into account, since the minima in γ are well defined.

4.2 The Separatrix Plane

For the study of phase transitions in the IBM-1 within the framework of catastrophe theory we already have the basic ingredients: the Hamiltonian of the system, Eq. (2.28), and the intrinsic state, Eq. (4.1). With them, the corresponding energy surface, Eq. (4.3) can be generated, in terms of the Hamiltonian parameters and the shape variables [22]. It is our purpose to find the values of the parameters of the Hamiltonian that correspond to critical points. In principle this analysis involves the 6 parameters of the Hamiltonian, but a first simplification occurs since the energy surface only depends on 5 parameters:

$$\left\langle c\left|\hat{H}\right|c\right\rangle = \frac{N\tilde{\varepsilon}\beta^2}{(1+\beta^2)} + \frac{N(N-1)}{(1+\beta^2)^2}\left(a_1\beta^4 + a_2\beta^3\cos(3\gamma) + a_3\beta^2 + \frac{u_0}{2}\right) \qquad (4.4)$$

where:

$$\left.\begin{aligned}
\widetilde{\varepsilon} &= \varepsilon_d + 6k_1 - \frac{9}{4}k_2 + \frac{7}{5}k_3 + \frac{9}{5}k_4 \\
a_1 &= \frac{1}{4}k_0 + \frac{1}{2}k_2 + \frac{18}{35}k_4 \\
a_2 &= 2\sqrt{2}\,k_2 \\
a_3 &= -\frac{1}{2}k_0 + 4k_2 \\
u_0 &= \frac{k_0}{2}
\end{aligned}\right\} \qquad (4.5)$$

Fortunately, it is possible to reduce the number of relevant (or essential) parameters to just two and study all phase transitions by using catastrophe theory.

4.3 Catastrophe Theory

The term catastrophe in mathematics, unlike the usual meaning as "*disaster*", means that smooth alterations in the controlling variables cause sudden changes in the phenomenon. It is originated by a French mathematician René Thom in the 1960s, catastrophe theory is a special branch of dynamical systems theory. It studies and classifies phenomena characterized by sudden shifts in behavior arising from small changes in circumstances [34].

In mathematical terms catastrophe theory means that small changes in the parameters of a system causes a sudden change in the function that describes the phenomenon. Natural phenomena are usually described by governing equations. Generally the equations are nonlinear, containing variables, constants, time and space coordinates, time and space derivatives of the variables, and of integral forms [34].

On the other hand, and in many cases, these equations can be simplified by assuming that they are of non-integral forms, and the problem can be

described by a set of partial nonlinear differential equations. Further assumptions can be made on the omission of the space coordinates and the space derivatives of the variables.

Catastrophes are bifurcations between different equilibria, or fixed-point attractors. Due to their restricted nature, classification of catastrophes can be based on how many control parameters are being simultaneously varied. For example, if there are two controls, then one finds the most common type, called a "*cusp*" catastrophe, as shown in Figure 4.1. If, however, there are move than five controls, there is no classification.

Catastrophe theory has been applied to a number of different phenomena, such as the stability of ships at sea and their capsizing, bridge collapse, and, with some less convincing success, the fight-or-flight behavior of animals and prison riots.

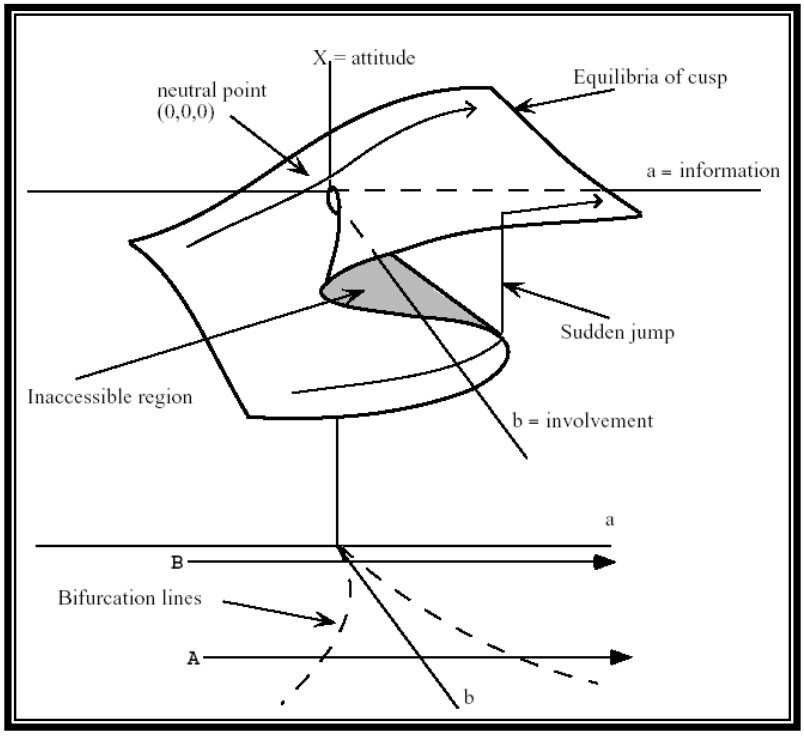

Figure 4.1: The cusp catastrophe model

References [32, 33] are refered for details of the application of catastrophe theory to the IBM-1case. The idea is to analyze the energy surface and obtain all equilibrium configurations, i.e. to find all the critical points of Eq. (4.4). First, the critical point of maximum degeneracy has to be identified. In our case, it corresponds to $\beta = 0$. Next, the bifurcation and Maxwell sets are constructed [32, 34]. Finally, the separatrix of the IBM-1 is obtained by the union of Maxwell and bifurcation sets.

In general a bifurcation set, corresponding to minima, limits an area where two minima in the energy surface coexist. A second order phase transition develops when these minima become the same. The crossing of a Maxwell set corresponding to minima leads to a first order phase transition.

In order to follow this scheme, one has to identify the catastrophe germ of the IBM-1, which is the first term in the expansion of the energy surface around the critical point of maximum degeneracy that cannot be cancelled by an arbitrary selection of parameters. In our case, one finds that the first derivative in $\beta = 0$ is always 0 because of the critical character of the point for any value of the parameters.

The second and third derivatives can also be canceled with an appropriate selection of parameters. However, if one imposes the cancellation of the fourth derivative, the energy becomes a constant for any value of β. This means that the catastrophe germ is β^4 and the number of essential parameters is equal to two, which can be defined, following reference [32, 33], as:

$$r_1 = \frac{a_3 - u_0 + \widetilde{\varepsilon}/(N-1)}{2a_1 + \widetilde{\varepsilon}/(N-1) - a_3} \tag{4.6}$$

$$r_2 = -\frac{2a_2}{2a_1 + \widetilde{\varepsilon}/(N-1) - a_3} \tag{4.7}$$

where $\widetilde{\varepsilon}$, a_1, a_2, and a_3 are defined in Eq.(4.5). The denominator in both expressions fixes the energy scale, which means that when it becomes negative, the energy surfaces are inverted.

The essential parameters r_1 and r_2 can also be written in terms of the parameters appearing in Eq. (2.28) as:

$$r_1 = \frac{\widetilde{\varepsilon} - (N-1)(k_0 - 4k_2)}{\widetilde{\varepsilon} + (N-1)(k_0 - 3k_2 + \frac{36}{35}k_4)} \tag{4.9}$$

$$r_2 = -\frac{4\sqrt{2}\, k_2 (N-1)}{\widetilde{\varepsilon} + (N-1)(k_0 - 3k_2 + \frac{36}{35}k_4)} \tag{4.10}$$

A property of the parametrization used in this work is that the different chains of isotopes are located on a straight line that crosses the point corresponding to the $U(5)$ limit. The equation of this line is given by:

$$r_1 = \frac{2k_0 - 7k_2 + \frac{36}{35}k_4}{4\sqrt{2}\, k_2} r_2 + 1 \tag{4.11}$$

It should be remarked that the derivation of the essential parameters has nothing to do with catastrophe theory. The application of this theory begins once those parameters are obtained.

The basic point is to translate every set of Hamiltonian parameters to the plane formed by the essential parameters r_1 and r_2. This plane is divided into several sectors by the bifurcation set, that form the geometrical place in the parameter space where $\frac{d^2E}{d\beta^2} = 0$ for a critical value of β, and the Maxwell sets, the geometrical place in the space of parameters where two or more critical points are degenerate [34].

Both sets form the separatrix of the system, in this case of the IBM-1. In References [40, 41] the IBM-1 bifurcation (r_2 axis, $r_2 = 0$ and $r_1 < 0$ semi-axis, r_{11}, and r_{12}) and Maxwell (negative r_1 semi-axis, r_{13}^{+}, and r_{13}^{-}) sets were obtained.

Chapter

5

Results, Discussion, Conclusions and Future Work

5.1 Results and Discussion

5.1.1 Fits

The best set of parameters for the Hamiltonian and $E2$ transition parameters for each isotopic chain are summarized in Tables (5-1) and (5-2).

Systematics of experimental and calculated energies for the states included in the least-square procedure is presented in order to show the goodness of the fitting procedure, as shown in Figures 5.1, 5.2, 5.3, and 5.4.

The experimental and calculated $B(E2)$ values are compared, good agreement were obtained for all chains as presented in Figures 5.5, 5.6, 5.7, and 5.8.

Finally, in Figure 5.9 the experimental and calculated S_{2n} values are shown. This is a fundamental magnitude for identifying a phase transition since it is directly related to the derivative of the energy surface. First order phase transitions are related with the appearance of a kink in the S_{2n} values. As shown in Figure 5.9, the calculation matches the experimentally observed behavior.

The analysis of the preceding figures for different observables and for several isotope chains shows that the present procedure is appropriate for systematic studies and confirms that it provides a simple framework to describe long chains of isotopes and detect possible phase transitions.

Table (5-1): Values of ε_d in the Hamiltonian (in keV) for each isotopic chain as a function of the neutron number.

Element	Neutron Number								
	84	86	88	90	92	94	96	98	100
$_{60}$Nd	1686.3	1606.7	1645.4	1602.9	1536.1	1595.9			
$_{62}$Sm	1427.3	1393.5	1289.3	1210.8	1158.6	1192.5	1312.2	1452.0	
$_{64}$Gd	1479.3	1508.7	1409.0	1300.4	1221.5	1174.4	1162.0	1176.5	
$_{66}$Dy	1558.8	1607.6	1562.4	1503.9	1461.0	1427.7	1413.4	1409.2	1443.1

Table (5-2): Rest of the parameters in the Hamiltonian and in the $E2$ transition operator.

Isotopes	$\widetilde{A}$ (MeV)	$\widetilde{B}$ (MeV)	k_0 (keV)	k_1 (keV)	k_2 (keV)	k_3 (keV)	k_4 (keV)	e_{eff} $(e.b)$	χ
$^{144-154}_{60}$Nd	16.75	-0.51	83.753	-13.928	-17.151	-101.27	-187.57	0.119	-1.43
$^{146-160}_{62}$Sm	18.05	-0.46	53.209	-11.267	-14.674	-31.769	-131.24	0.119	-1.69
$^{148-162}_{64}$Gd	22.55	-0.76	45.207	-7.932	-13.129	-35.224	-156.24	0.110	-1.77
$^{150-166}_{66}$Dy	25.06	-0.80	38.651	-6.416	-13.638	-59.165	-163.05	0.103	-1.60

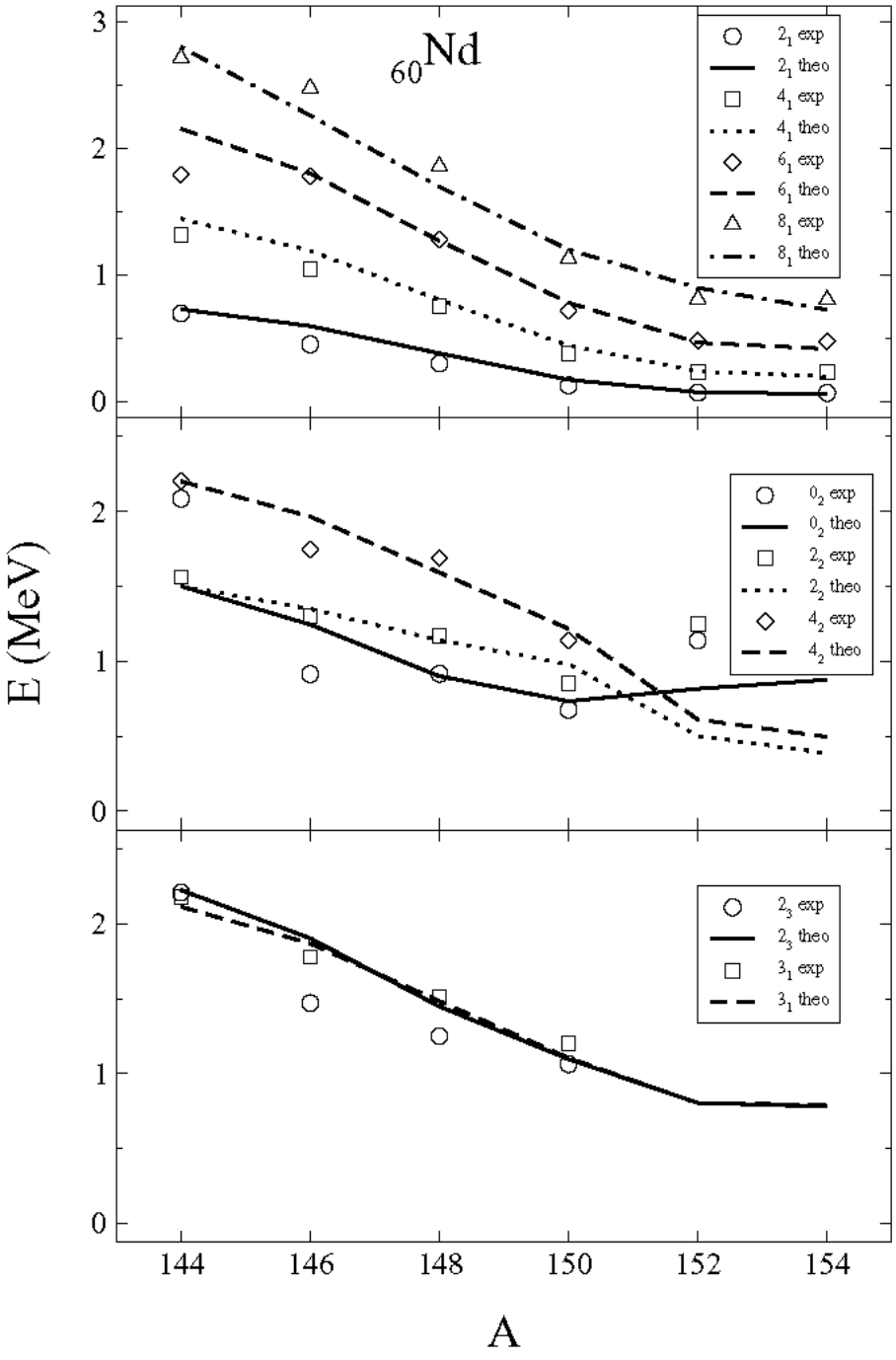

Figure 5.1: Excitation energies of Nd isotopes.

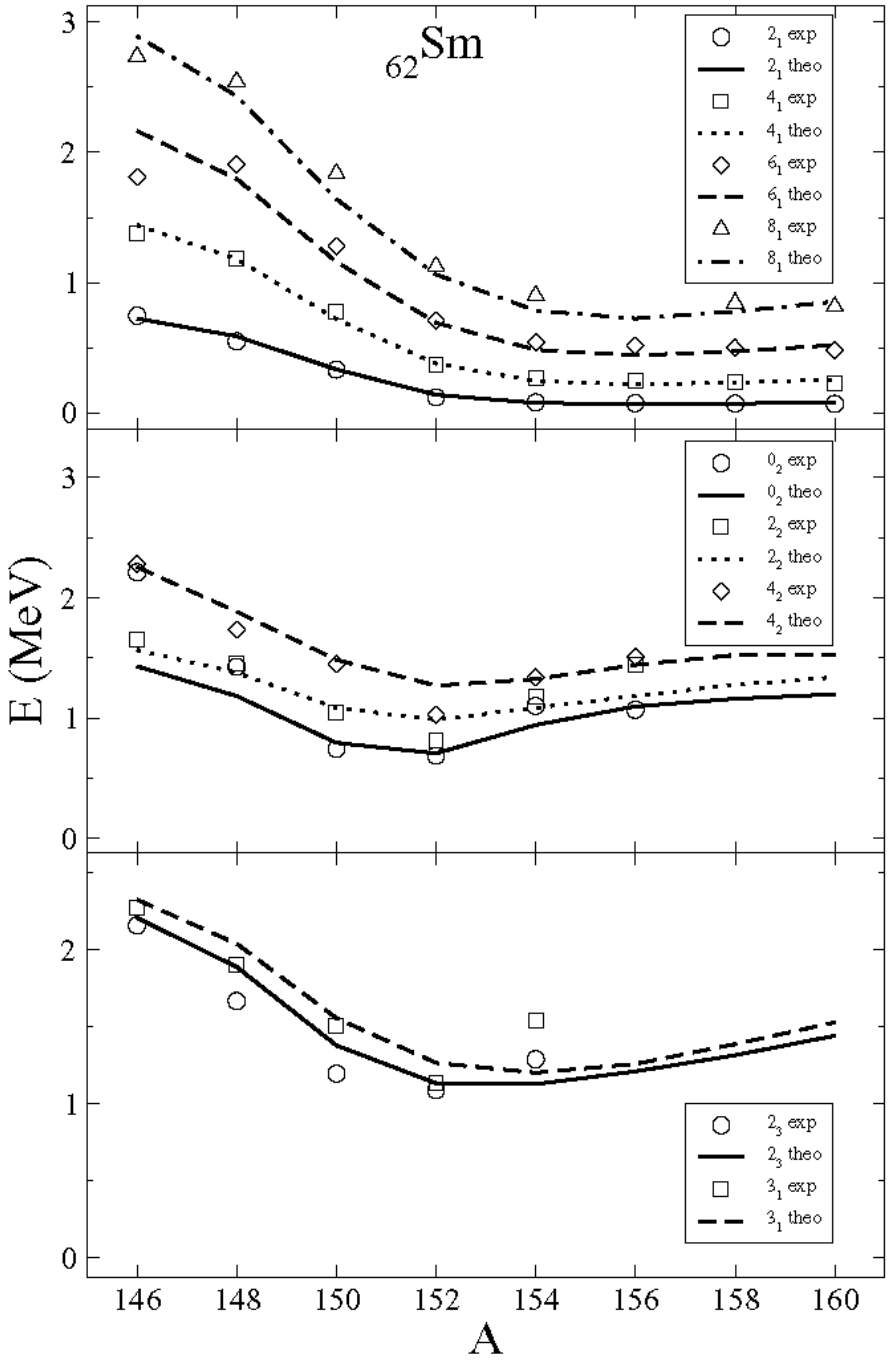

Figure 5.2: Excitation energies of Sm isotopes.

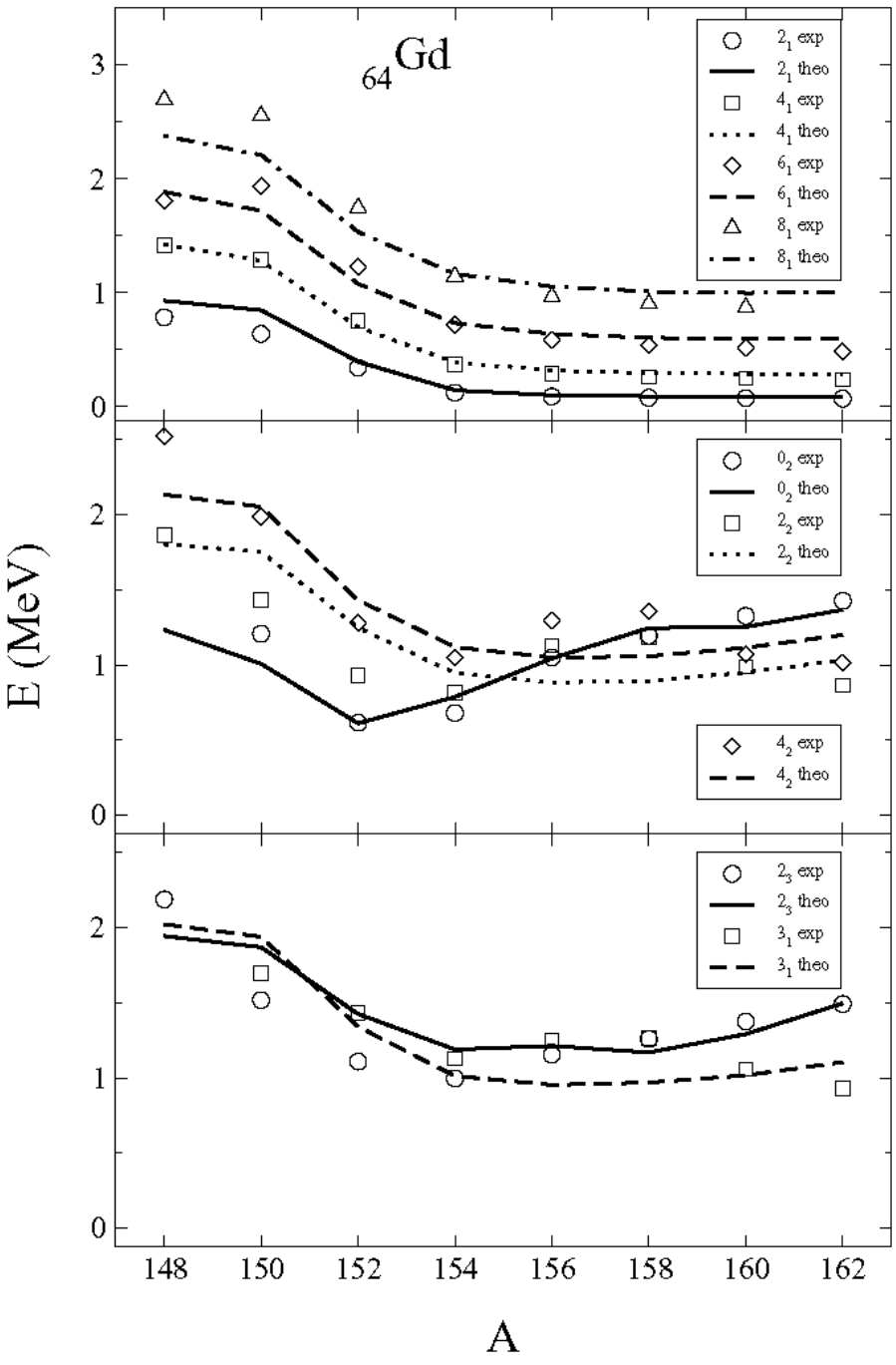

Figure 5.3: Excitation energies of Gd isotopes.

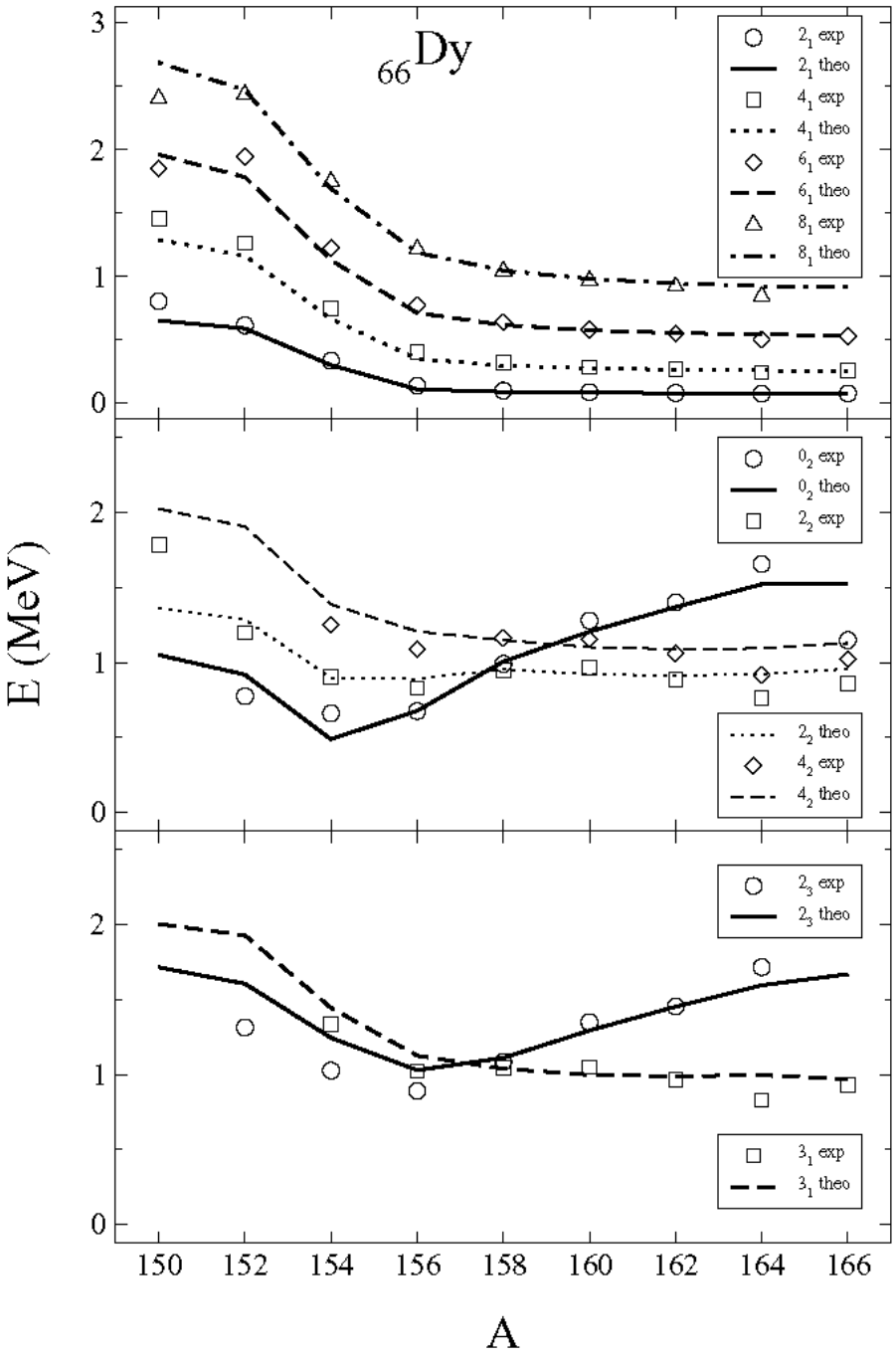

Figure 5.4: Excitation energies of Dy isotopes.

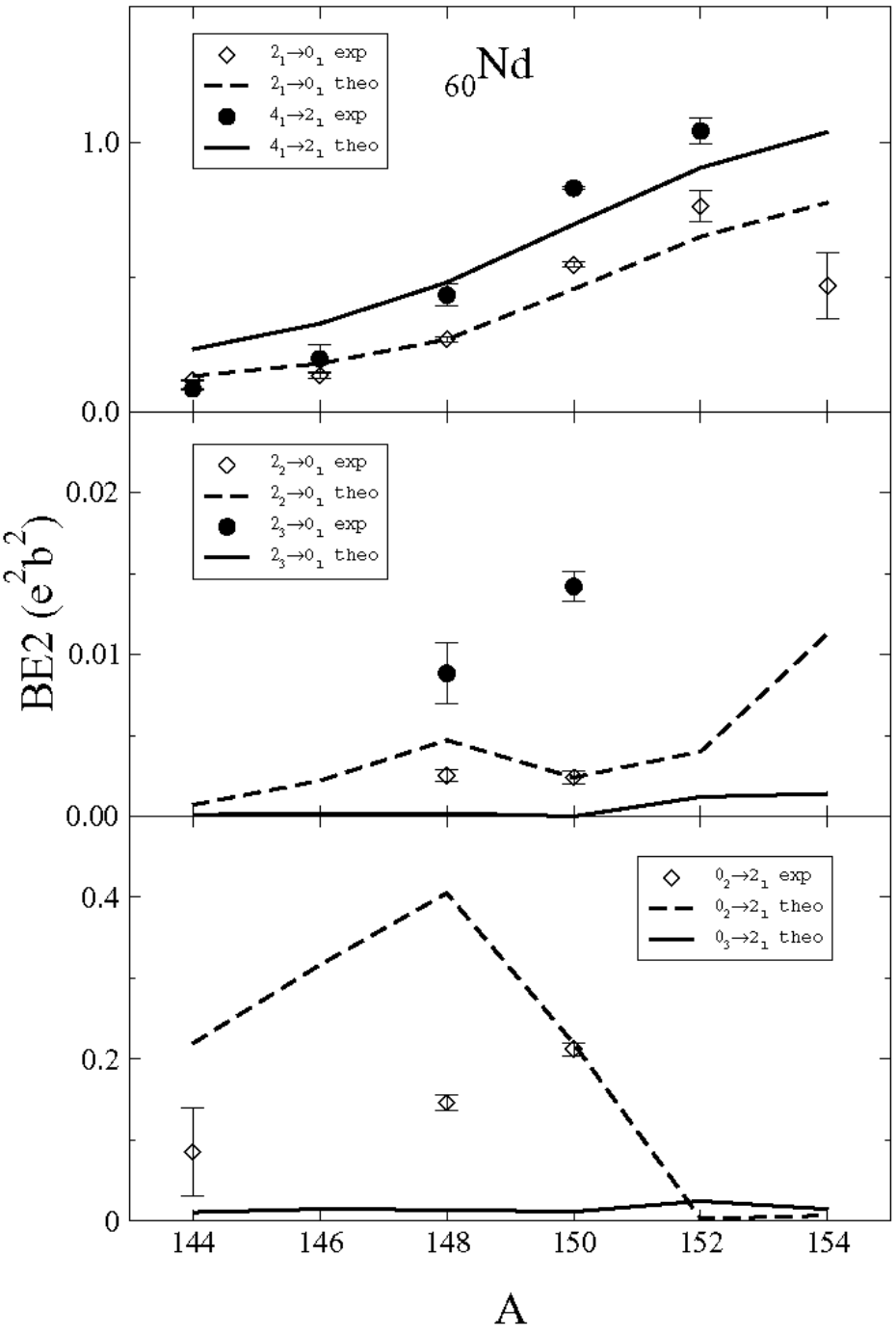

Figure 5.5: *B*(*E*2) transition rates for Nd isotopes.

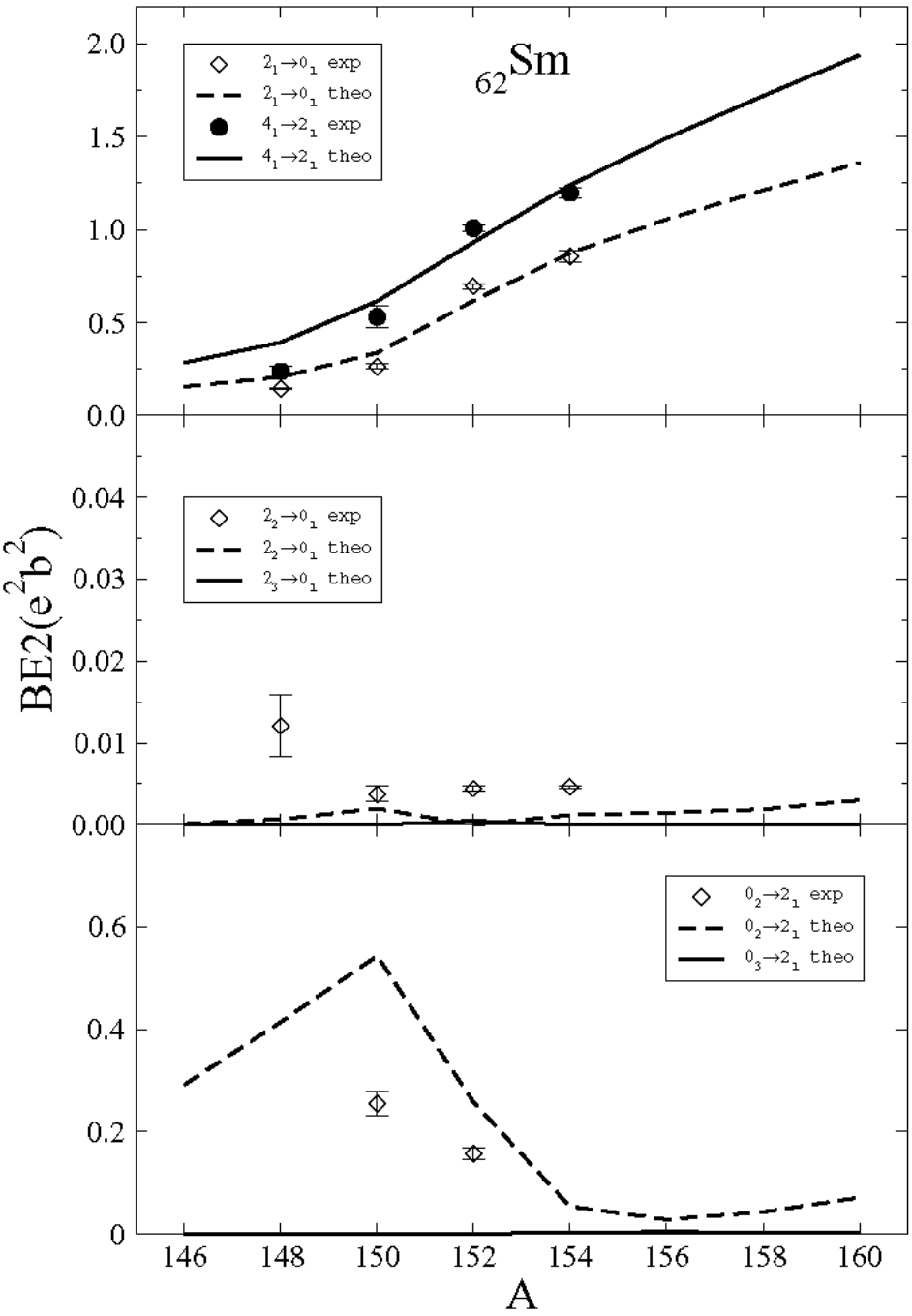

Figure 5.6: *B*(*E*2) transition rates for Sm isotopes.

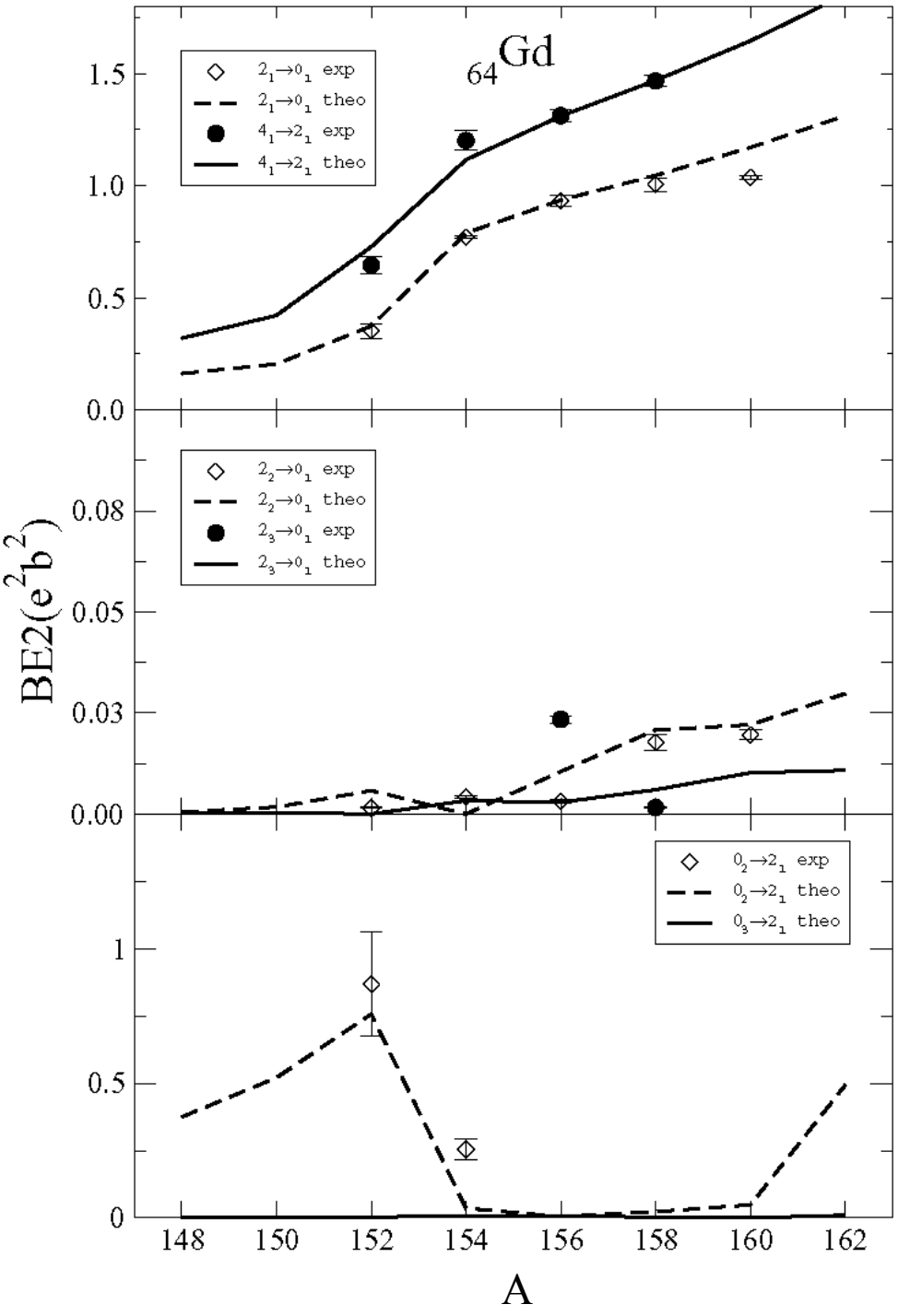

Figure 5.7: $B(E2)$ transition rates for Gd isotopes.

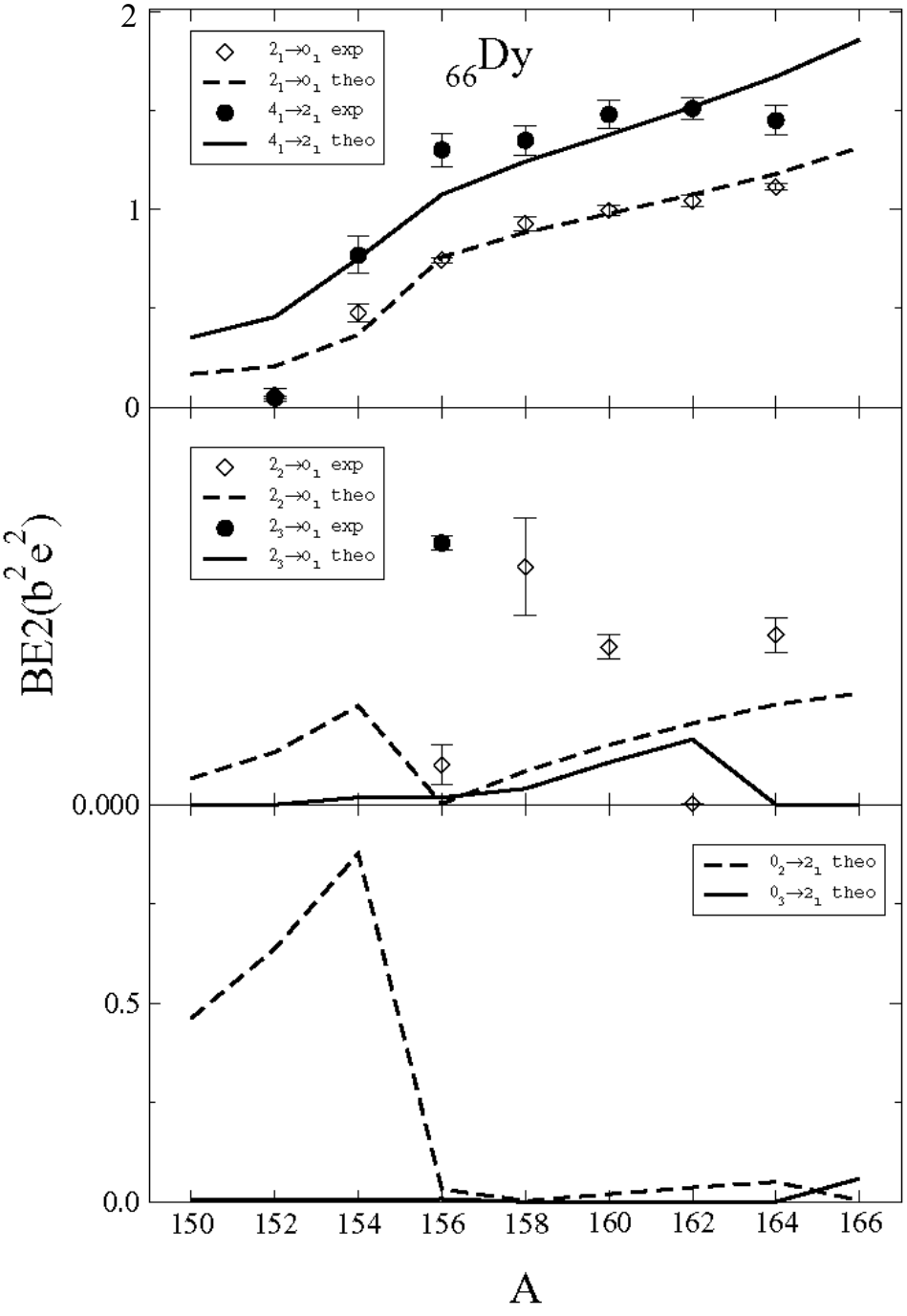

Figure 5.8: *B*(*E*2) transition rates for Dy isotopes.

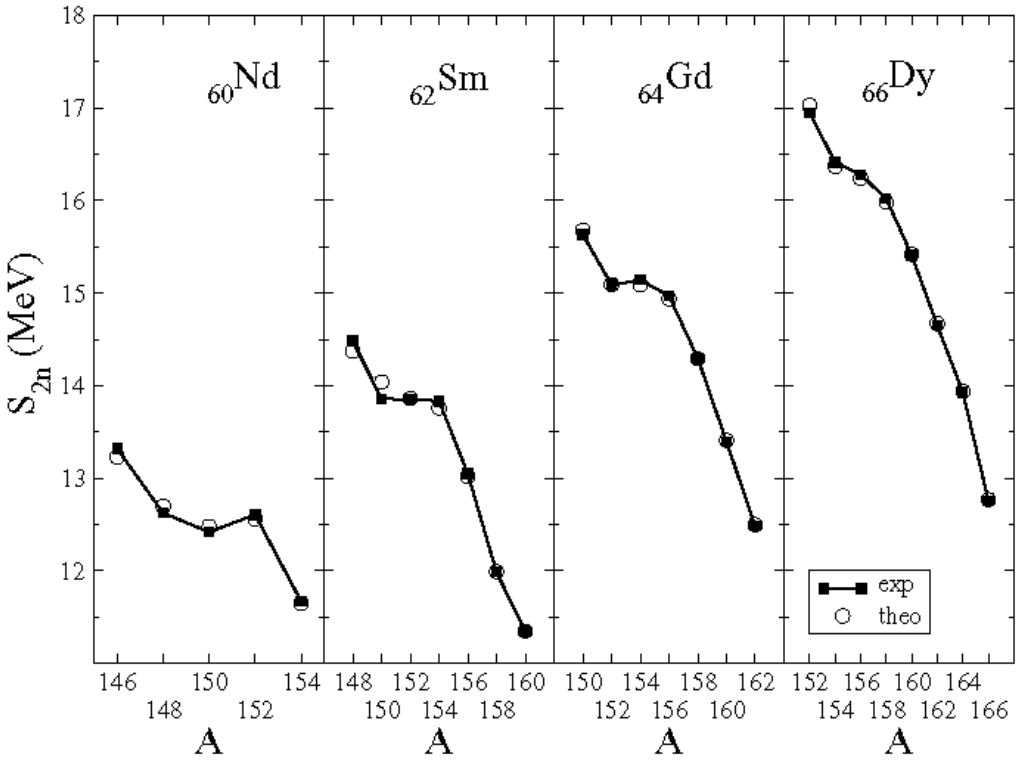

Figure 5.9: S_{2n} values for Nd, Sm, Gd, and Dy isotopes.

The relevant transition rates for ^{152}Sm were calculated in this work and compared with the recent experimental data, the work of $X(5)$ Ref. [7] and CQF work Ref. [4] as in the present work, they compare the experimental and theoretical values for excitation energies and $B(E2)$ transition rates. The transition rates $B(E2)$ may be written in Weiskopf units (W.u.) [58]. Both methods provide a consistent description of the rare-earth region with a similar number of parameters as can be observed in Figure 5.10 and in Table (5-3).

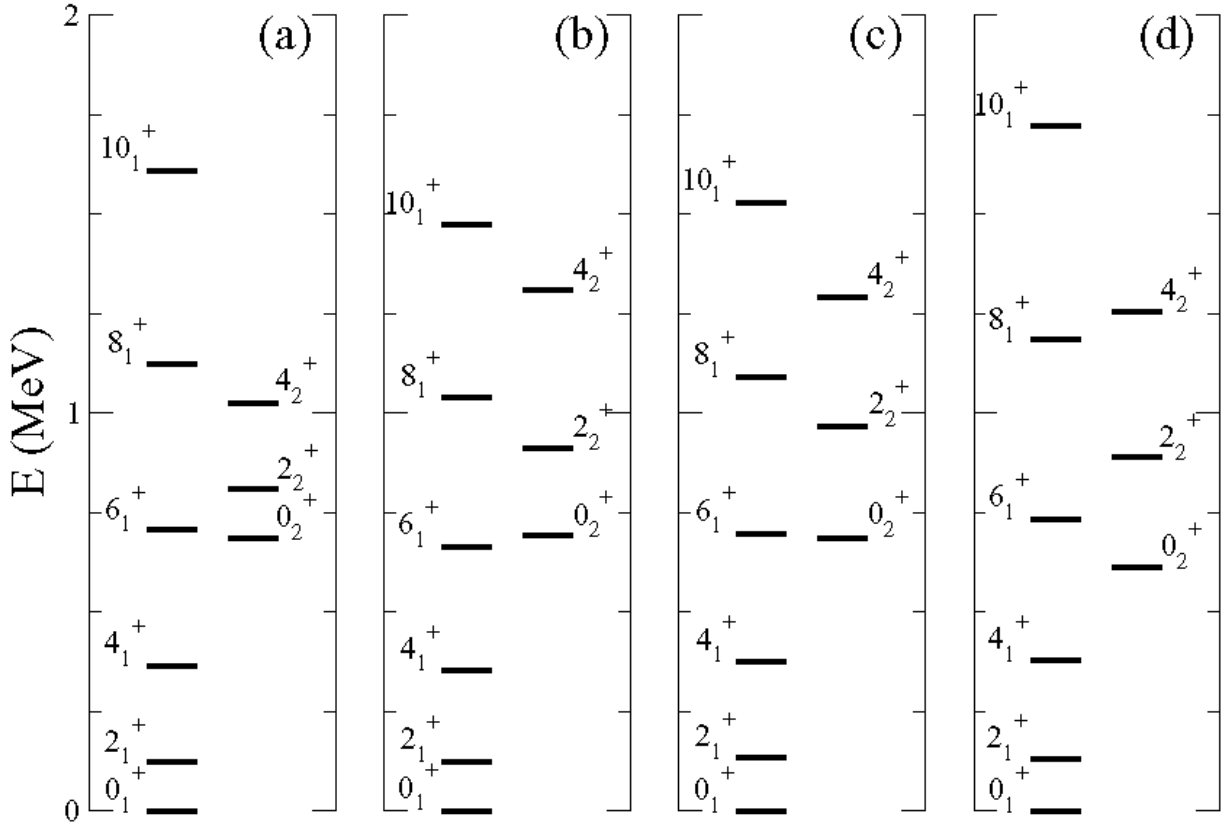

Figure 5.10: Spectrum of ^{152}Sm: (a) experimental [56], (b) $X(5)$ symmetry [7], (c) this work, and (d) using CQF [4].

Table (5-3): Relevant transition rates for ^{152}Sm (in W.u.).

$B(E2)$	Exp.[a]	$X(5)$[b]	This Work	CQF[c]
$B(E2: 2_1^+ \to 0_1^+)$	144	144	144	144
$B(E2: 4_1^+ \to 2_1^+)$	209	228	210	216
$B(E2: 6_1^+ \to 4_1^+)$	245	285	227	242
$B(E2: 8_1^+ \to 6_1^+)$	285	327	317	248
$B(E2: 10_1^+ \to 8_1^+)$	320	376	318	242
$B(E2: 0_2^+ \to 2_1^+)$	33	91	24	57
$B(E2: 2_2^+ \to 4_1^+)$	19	52	14	20
$B(E2: 2_2^+ \to 2_1^+)$	6	13	5	11
$B(E2: 2_2^+ \to 0_1^+)$	1	3	0.1	0.1
$B(E2: 4_2^+ \to 6_1^+)$	4	40	7	14
$B(E2: 4_2^+ \to 4_1^+)$	5	9	2	8
$B(E2: 4_2^+ \to 2_1^+)$	1	13	0	0.1

[a] Taken from Ref. [57], [b] Following Ref. [7] and [c] Following Ref. [4].

5.1.2 Energy surface and phase transition

In Figure 5.11 the energy surfaces for the isotopes of the different isotope chains studied in this thesis are plotted as a function of β. The Figure on the right is a zoom of the region close to $\beta = 0$. The classification of phase transitions that we follow in this thesis and that is followed traditionally in the IBM-1 is the Ehrenfest classification [65]. In this context, the origin of a phase transition resides in the way the energy surface (their minima positions) is changing as a function of the control parameter that, in this work, is a combination of parameters of the Hamiltonian. First order phase transitions appear when there exists a discontinuity in the first derivative of the energy with respect to the control parameter. This discontinuity appears when two degenerate minima exist in the energy surface for two values of the order parameter β. Second order phase transitions appear when the second derivative of the energy with respect to the control parameter displays a discontinuity. This happens when the energy surface presents a single minimum for $\beta = 0$ and the surface satisfies the condition $\left(\frac{d^2E}{d\beta^2}\right)_{\beta=0} = 0$.

With the introduction of the $E(5)$ and $X(5)$ symmetries to describe phase transitional behavior, diverse attempts to identify nuclei that could be located at the critical points have been made. The theoretical approaches have been mainly performed with restricted IBM-1 Hamiltonians. In particular, within the CQF, or other restricted Hamiltonians, the location of the critical point is obtained by imposing $\frac{d^2E}{d\beta^2} = 0$ at $\beta = 0$, where E is the energy surface [4]. This condition leads to a flat surface in a region of small values of β, with a single minimum in the limit $\chi = 0$ and two almost degenerate minima (one of them in $\beta = 0$) in the

other cases. In the CQF approximation it can be said that $\left(\frac{d^2E}{d\beta^2}\right)_{\beta=0}=0$ corresponds approximately to a "*very flat energy surface*" as happens for the $E(5)$ and $X(5)$ critical point models. Following this approach both ^{150}Nd and ^{152}Sm have been found to be close to critical. However, when studying a transitional region in which the lighter nuclei are spherical and the heavier are well deformed, the priori restriction of the parameter space could play a crucial role in the identification of a particular isotope as critical. Thus, it is important to perform a general analysis in order to check whether the predictions obtained within the CQF for those nuclei close to a critical point are robust.

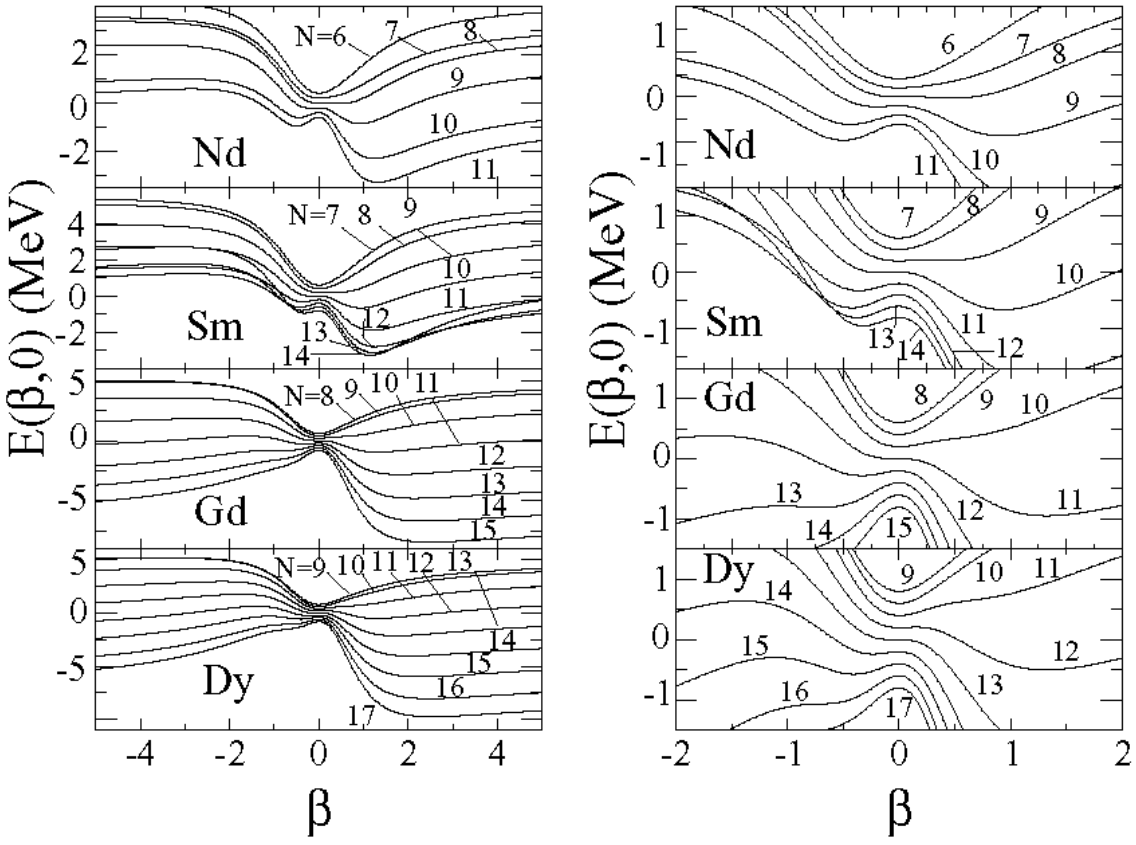

Figure 5.11: Energy surfaces for the different chain of isotopes.

5.1.3 Separatrix plane

All Maxwell sets are indicated in Figure 5.12. In this representation it is required that the denominator in Eq. (4.6) and Eq. (4.7) is positive. The separatrix for $r_1 > 0$ is associated to minima while for $r_1 < 0$ is associated to maxima (except the negative r_1 semi-axis). In order to clarify the Figure on the separatrix, the energy surfaces corresponding to each set are plotted as insets. The half plane with $r_2 > 0$ corresponds to prolate nuclei, while the one with $r_2 < 0$ corresponds to oblate nuclei. Note that Eq.'s (4.9) and (4.10) are only valid for prolate nuclei, but can be readily obtained for the oblate case. On this Figure the symmetry limits and the correspondence with Casten's triangle [9] are also represented. For completeness one should consider the case where the denominator of Eq. (4.6) and Eq. (4.7) is negative. It implies that the energy scale becomes negative and the energy surface should be inverted. The separatrix for this case is plotted in Figure 5.13 and corresponds to the inversion of Figure 5.12. Again the schematic energy surfaces corresponding to each branch of the separatrix are shown as insets. Note that in this case the symmetry limits do not appear in the Figure because they correspond to positive denominators for r_1 and r_2. In our analysis only prolate nuclei are considered, because of that a new Figure, Figure 5.14, is included. In this Figure, the right panel corresponds to positive denominators for r_1 and r_2 while the left panel shows the case of negative denominator for r_1 and r_2. In the following we will follow the convention presented in this Figure.

A set of parameters in the Hamiltonian corresponds to a point in the separatrix plane. The location of the point in that plane provides the required information on its transitional phase character. As mentioned in chapter 4, it follows that points located on a separatrix line correspond to critical points. Note

that the dynamical behavior of the system is controlled by the lowest minimum in the energy surface. In this sense we are adopting the Maxwell convention in the catastrophe theory language [38] and the only relevant branches of the separatrix are r_{13}^{+} and $r_2 = 0$ with $r_1 \leq 0$. All these branches correspond to first order phase transitions except for the single point ($r_1 = 0$, $r_2 = 0$) that corresponds to a second order phase transition. The rest of Maxwell lines do not correspond to a phase transition because they are related to maxima. The interest of the bifurcation set, corresponding to minima, arises from the fact that it defines regions where two minima exist.

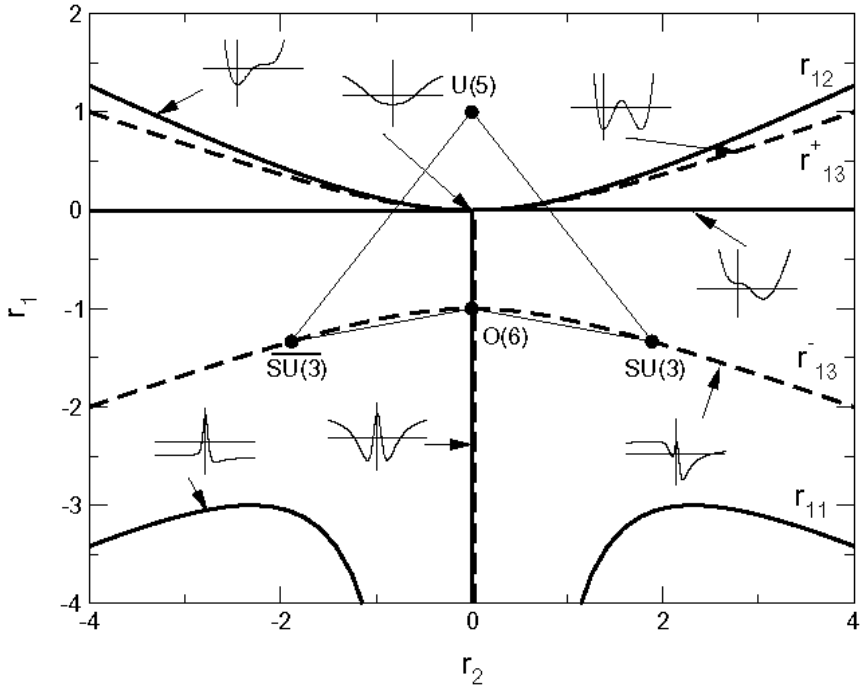

Figure 5.12: Separatrix plane with a positive energy scale.

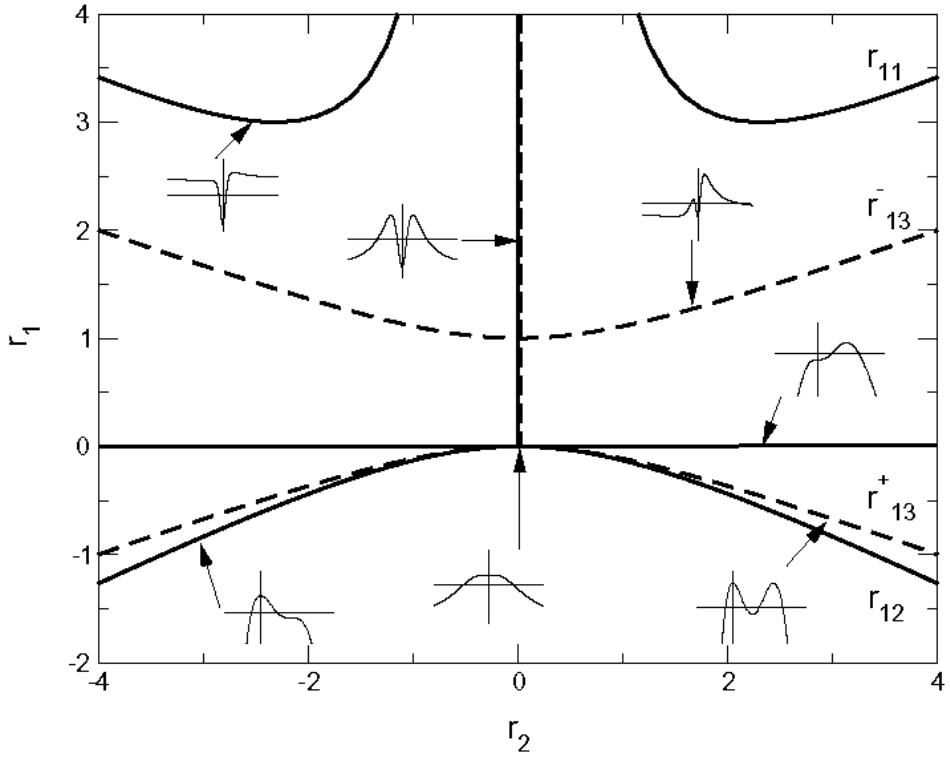

Figure 5.13: Separatrix plane with a negative energy scale.

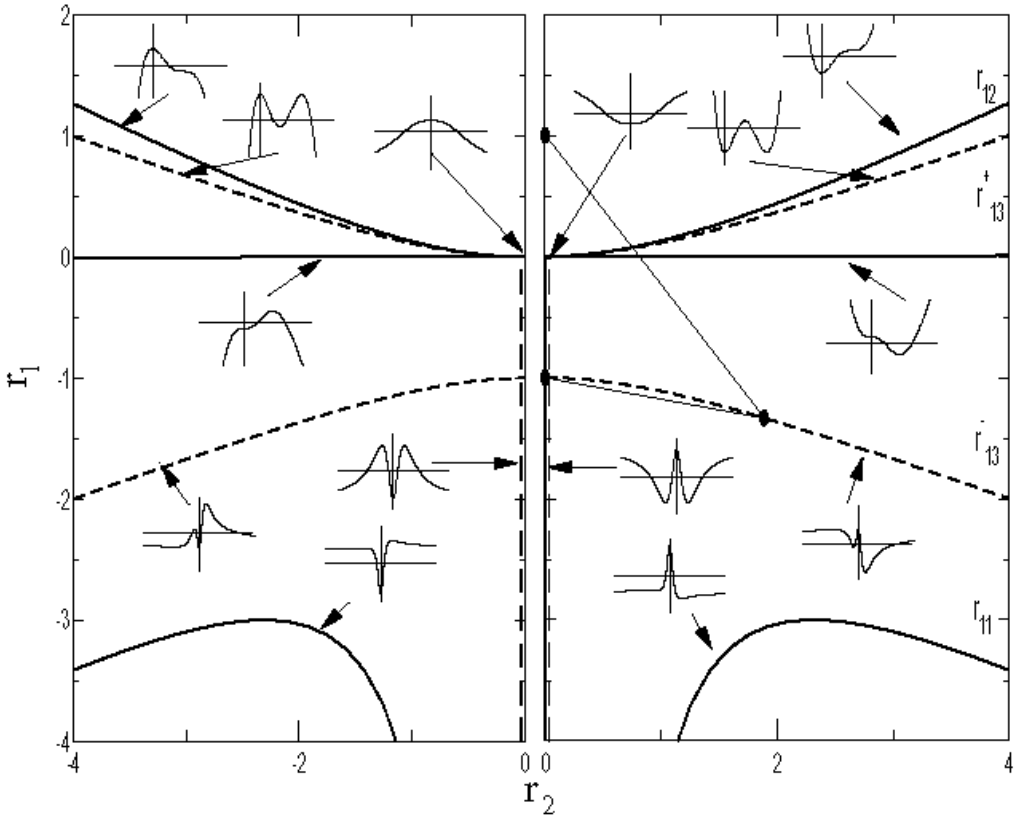

Figure 5.14: Separatrix plane for prolate nuclei ($\chi < 0$).

5.1.4 Rare-earth region on the separatrix plane

The fits presented in Chapter 3 provide the parameter sets given in Tables (5-1) and (5-2) for the four isotope chains studied in this work. In this section we plot the corresponding sequences of points representing the isotopes in each chain on the separatrix plane. As can be observed in the previous tables all the parameters for each chain are fixed except the value of ε_d that changes along the chain.

In Figure 5.15 the positions of the different isotopes in the chains studied are plotted in the separatrix plane. The interpretation of these lines is given in Figure 5.14. As mentioned above, all isotopes in a chain lie on a straight line. The lighter ones are close to the $U(5)$ point (spherical shapes) while as the number of neutrons is increased the corresponding points get increasingly away. For the heavier isotopes of Gd, and Dy the denominator of r_1 and r_2 becomes negative, which means that the left panel in Figure 5.14 has to be used.

The main feature for some nuclei is close to the Maxwell set r_{13}^{+}: the closest are ^{148}Nd (boson number $N = 8$) and ^{150}Sm (boson number $N = 9$) and not far away ^{152}Gd (boson number $N = 10$). This can be complemented with the image of the energy surfaces plotted in Figure 5.11. The energy surface for ^{148}Nd and ^{150}Sm are rather flat around $\beta = 0$. For ^{152}Gd the situation is not so clear. For Dy there is no isotope close to the critical point.

According to our calculations, the transition from spherical to deformed shapes occurs between $N = 11$ and $N = 12$. The isotope ^{162}Dy is close to the Maxwell set but in the left panel. In this situation there should be two degenerate maxima. This can be observed in the corresponding energy surface (boson number $N = 15$) in Figure 5.11. The isotopes ^{150}Nd ($N = 9$) and ^{152}Sm ($N = 10$)

(also can be included in this situation ^{154}Gd (N = 11) and ^{158}Dy (N = 13)) are close to the bifurcation set r_2 axis. Again inspection of Figure 5.11 shows that the energy surfaces for these isotopes has a minimum for $\beta > 0$ and a maximum at $\beta = 0$.

In Figure 5.16 we show an amplification of the critical area. In conclusion, from this global analysis, it is found that ^{148}Nd, ^{150}Sm, and (less clearly) ^{152}Gd, are close to criticality. These isotopes are quite close but do not exactly coincide with previously proposed critical nuclei ^{150}Nd and ^{152}Sm [66, 17], where the quite basic criterion was the closeness of their low-lying excitation spectra and transition intensities with the $X(5)$ values.

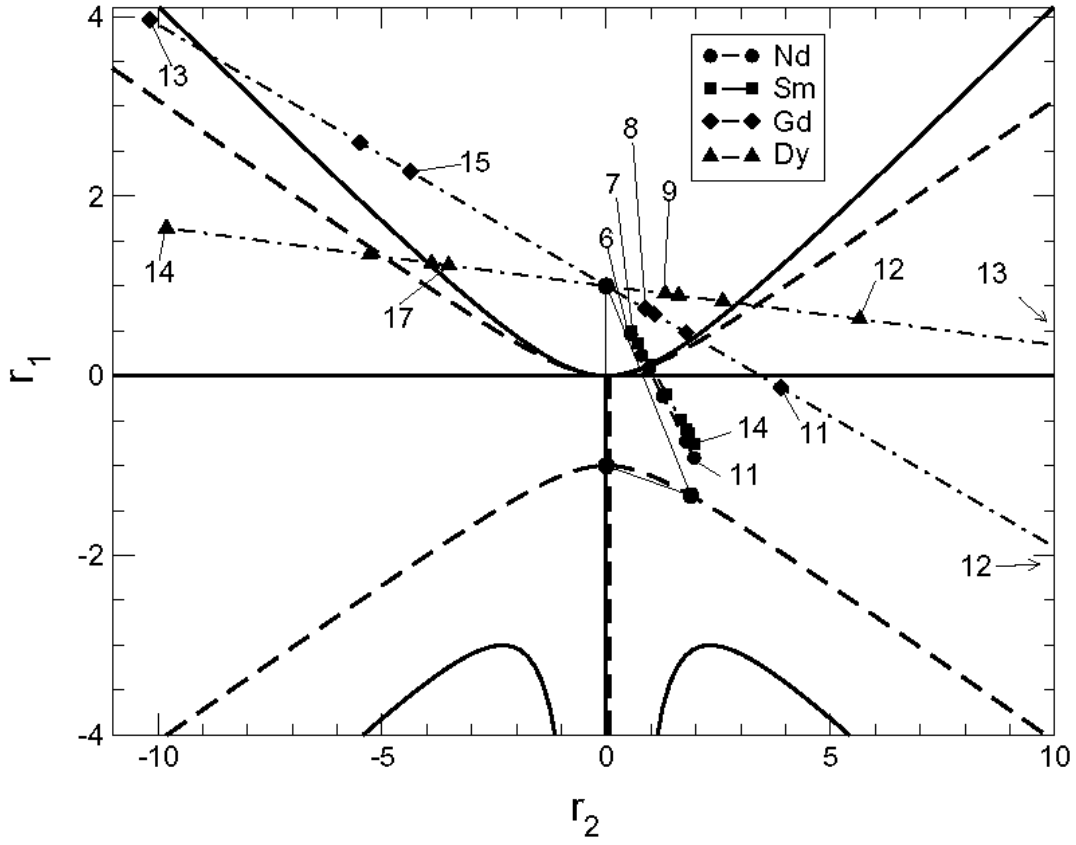

Figure 5.15: Representation of isotopes in the separatrix plane (with $\chi < 0$). The numbers on the isotopes correspond to the number of bosons.

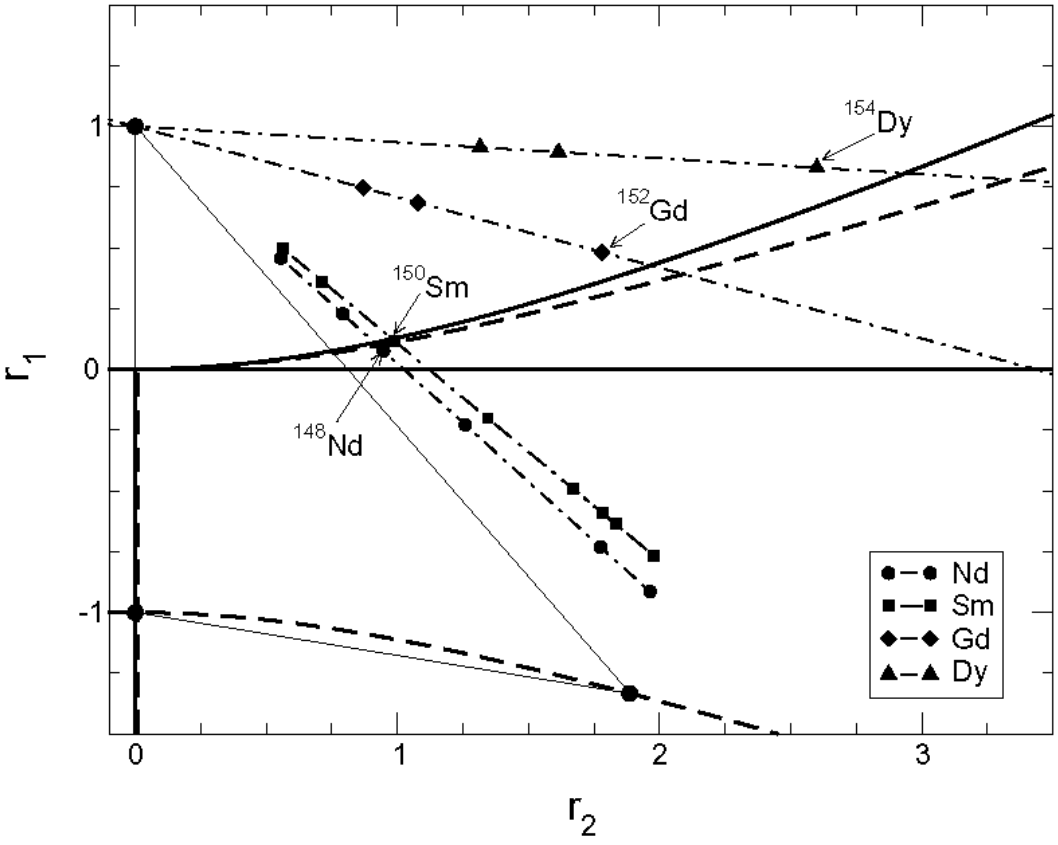

Figure 5.16: Representation of isotopes in the separatrix plane in a closest view.

5.1.5 Prediction of critical points within CQF

The CQF uses a simplified Hamiltonian with only three parameters. For the description of transitional nuclei from the $U(5)$ to the $SU(3)$ limits the parameters are allowed to vary nucleus by nucleus.

The representation of such calculations in the separatrix plane shows that all isotopes in a chain are basically on top of the straight line connecting the $U(5)$ point, $(r_1, r_2) = (1, 0)$, and the $SU(3)$ point, $(r_1, r_2) = (-4/3, 4\sqrt{2}/3)$. Note that this point corresponds strictly to the $SU(3)$ Casimir operator.

However, a more general CQF $SU(3)$ Hamiltonian still lies very close to the latter point. In general, the same happens in the $U(5)$ and $O(6)$ points. This means that within this framework the exploration of only a limited area in the separatrix plane is allowed. If all isotopes in an isotopic chain are forced to be located on the line connecting the $U(5)$ and $SU(3)$ points, it follows that one will more often find an isotope close to the (unique) critical point. In the calculations presented here we have seen that within the general formalism this is not always the case. For example, for Dy we did not find an isotope close to a critical point. In previous systematic studies in the rare-earth region using the CQF formalism, Ref. [42] and [40], the corresponding energy surfaces were not presented.

We have constructed them from the parameters given in those references and the results obtained are consistent with those given in the present work. In particular, ^{148}Nd and ^{150}Sm seem to be closest to a critical point.

5.2 Conclusions

In this dissertation we have analyzed chains of isotopes in the rare-earth region. In these chains nuclei evolve from spherical to deformed shapes. We have performed an analysis of the corresponding shape transitions to look for possible nuclei at or close to a critical point. We have used the more general one- and two- body IBM-1 Hamiltonian and generated energy surfaces using the coherent state formalism. We have then used catastrophe theory to classify phase transitions and to decide if a nucleus is close to criticality.

The approach used to fix the Hamiltonian parameters leads to a very good global agreement with the experimental data corresponding to excitation energies, $B(E2)$'s and S_{2n} values. In particular, an excellent agreement with the measured S_{2n} values is obtained, which is considered a key observable to locate phase transitional regions. The analysis presented here is consistent with previous CQF studies in the same region. As a result we find that ^{148}Nd and ^{150}Sm are the best candidates to be critical, but we should remark that ^{150}Nd and ^{152}Sm are not far away from it.

A possible new way of defining critical nuclei is based on the "*critical symmetries*" $E(5)$ or $X(5)$ [7, 8]. The properties associated with these solutions allow the identification of critical points by comparing the experimental data with characteristic energy and transition rate ratios. Thus, it may be possible to decide whether a nucleus is critical by analyzing its spectrum and decay properties. A question may be arise here, whether a flat energy surface can be truly associated to a given nucleus with energy ratios close to $X(5)$. A clear example is ^{152}Sm; we have shown that according to our study the IBM-1 energy surface of this nucleus is not so flat as expected from previous analyses, i.e. in our work, it does not correspond to a critical point as suggested earlier. However,

if the spectrum and transition rates are analyzed (see Figure 5.10 and Table (5-3)), this nucleus reproduces reasonably well the main $X(5)$ features. We note that in the general IBM-1 framework there is no unique spectrum associated to a given potential energy surface, as implied by Eq.'s (4.6) and (4.7). Catastrophe theory constitutes a definite criterion regarding this issue, but does not provide a measurable signature in itself.

5.3 Future work

It seems clear that further work is required to find more identifiable features which signal criticality in an unequivocal way. This work can be repeated but instead of letting ε_d changes from isotope to isotope, fix the value of ε_d and change the structure parameter χ from $0 \rightarrow 1$ along the leg from $U(5)$ to $SU(3)$ limits and from $0 \rightarrow -1$ along the leg from $U(5)$ to $\overline{SU(3)}$ limits.

The present calculations can be performed in the framework of proton-neutron Interacting Boson Model (IBM-2) which may enhance the calculations and leads to best results to identify the critical points in these chains of isotopes.

Appendix A

The code PHINT calculates energies of nuclear states and reduced transition probabilities of the electromagnetic radiation in the interacting boson model (IBM-1). It was written by O. Scholten in FORTRAN language, published in Computational Nuclear Physics Ref. [43].

The IBM-1 calculations can be performed in the basic form of the Hamiltonian Eq. (2.28) with program PCIBAXW. The input parameters (in capitals in the block below) correspond to the following coefficients in Eq. (2.28).

ε_d	HBAR
k_0	K(0)
k_1	K(1)
k_2	K(2)
k_3	K(3)
k_4	K(4)

The technical notes of O. Scholten (1991, p.88) the following remarks have to be added [44]:

- The subroutine RDPAR in the packet PCIBALIB has to be corrected in order to enable it to read the input parameters as triplet (for example (3F10.4) has to be replaced by (3F7.4)).
- Energies should be given in MeV.
- In order to compile the source program no sensitive debug can be used (for example for the FORTRAN compiler of Microsoft only the command fl and not fl/4YP must be given).
- Increasing the boson number N to 14 or 16 calls for changes in COMMON (READMAT) and in the corresponding DATA in various places of the programs.

Appendix B

B.1 Basic definitions

A group G is a set of distinct elements, for which a law of composition (such as addition, multiplication, matrix multiplication, etc.) is well defined, and which satisfies the following criteria [67]:

1. If G_1 and G_2 are the elements of G, then their composition $G_3 = G_1 \cdot G_2$ is also an element of G.
2. The composition law is associative: $(G_1 \cdot G_2) \cdot G_3 = G_1 \cdot (G_2 \cdot G_3)$
3. There exists an identity element E such that $E \cdot G = G \cdot \mathrm{E} = G$ for each element G.
4. For each element G from **G**, there exists a unique inverse element G^{-1}such that $G^{-1} \cdot \mathrm{G} = G \cdot G^{-1} = E$.

- The number of group elements is called the *order* of the group.
- A group containing a finite number of elements is called a *finite* group.
- A group containing an infinite number of elements is called an *infinite* group.
- An infinite group can be discrete or continuous.
- If the number of group elements is denumerably infinite, the group is called discrete.
- If the number of group elements is non-denumerably infinite, the group is called continuous.

In general, the product $G_1 \cdot G_2$ does not have to equal $G_2 \cdot G_1$. However, if $G_1 \cdot G_2 = G_2 \cdot G_1$, the group is called *abelian*.

B.2 Point symmetry groups

The transformations which preserve the distances between the points and bring the body into coincidence with itself are called *symmetry transformations*. All symmetry transformations form a *symmetry group* of the body. The symmetry groups of finite bodies which leave at least one point of the body fixed are called *point symmetry groups*.

All point symmetry groups consist of three fundamental operations [67]:

- Rotations through an angle $2\pi/n$, (n is integer) around a certain axis: C_n.
- Reflection in a symmetry plane: σ;
- Combined rotation through an angle $2\pi/n$, (n is integer) around a certain axis and reflection in the perpendicular plane: $S_n = C_n\ \sigma_h$

B.3 Symmetric group

All permutations of n identical objects [68]:

$$\begin{pmatrix} 1 & 2 & 3 & \dots & n \\ p_1 & p_2 & p_3 & \dots & p_n \end{pmatrix} \tag{B.3.1}$$

Form a group called a *symmetric group* of degree n, denoted as S_n. The group contains $n!$ elements.

B.4 General linear group

B.4.1 GL(2)

The linear group in two dimensions GL(2) is a group of all linear transformations of two coordinates (x , y),

$$\begin{aligned} x' &= a_{11}x + a_{12}y \\ y' &= a_{21}x + a_{22}y \end{aligned} \qquad \text{(B.4.1.1)}$$

where the parameters a_{11}, a_{12}, a_{21} and a_{22} as well as the coordinates x and y can be complex and for which the determinant

$$\begin{vmatrix} a_{11} & a_{12} \\ a_{21} & a_{22} \end{vmatrix} \neq 0 \cdot \qquad \text{(B.4.1.2)}$$

The transformation (5) can be re-written in a matrix form.

$$\begin{pmatrix} x' \\ y' \end{pmatrix} = \begin{pmatrix} a_{11} & a_{12} \\ a_{21} & a_{22} \end{pmatrix} \begin{pmatrix} x \\ y \end{pmatrix} \qquad \text{(B.4.1.3)}$$

Thus, we can give an equivalent definition: GL(2) is a group formed by all regular complex (2×2) matrices.

The group is characterized by eight real parameters (or four complex parameters a_{11}, a_{12}, a_{21} and a_{22}).

B.4.2 GL(n)

All regular complex ($n \times n$) matrices form the *general linear group* GL(n), which is characterized by $2n^2$ real parameters.

The group GL(n) is a non-compact group.

B.5 Unitary groups

B.5.1 U(2)

The linear transformations in two dimensions can be read as [68]:

$$\begin{aligned} x' &= a_{11}x + a_{12}y \\ y' &= a_{21}x + a_{22}y \end{aligned} \tag{B.5.1.1}$$

with

$$\begin{vmatrix} a_{11} & a_{12} \\ a_{21} & a_{22} \end{vmatrix} \neq 0 \cdot \tag{B.5.1.2}$$

satisfy the additional condition:

$$|x'|^2 + |y'|^2 = |x|^2 + |y|^2 \cdot \tag{B.5.1.3}$$

From (B.5.1.3), the parameters a_{ij} should obey the following relations:

$$\begin{aligned} &|a_{11}|^2 + |a_{12}|^2 = 1, \\ &|a_{21}|^2 + |a_{22}|^2 = 1, \\ &a_{11}a_{12}^* + a_{21}a_{22}^* = 0. \end{aligned} \tag{B.5.1.4}$$

All such transformations form a unitary group in two dimensions U(2).

An equivalent definition: U(2) is a group formed by all regular unitary (2×2) matrices.

The group is characterized by four real parameters.

B.5.2 U(n)

All unitary ($n \times n$) matrices form the n^2 -parameter *unitary group* U(n).

The group U(n) is a subgroup of the group GL(n).

The group U(n) is a compact group since $\left|a_{ij}\right|^2 \leq 1$.

B.5.3 SU(n)

All unitary ($n \times n$) matrices whose determinants are equal to +1 form the (n^2-1) parameter *special unitary group* SU(n).

The group SU(n) is a subgroup of the group U(n).

B.6 Orthogonal groups

B.6.1 O(2)

The linear transformations in two dimensions, which preserve the distance between two-points is:

$$\begin{aligned} x' &= a_{11}x + a_{12}y \\ y' &= a_{21}x + a_{22}y \end{aligned} \qquad \text{(B.6.1.1)}$$

where the parameters a_{11}, a_{12}, a_{21} and a_{22} as well as the coordinates x and y take only real values,

$$\begin{vmatrix} a_{11} & a_{12} \\ a_{21} & a_{22} \end{vmatrix} \neq 0 \cdot \qquad \text{(B.6.1.2)}$$

and

$$x'^2 + y'^2 = x^2 + y^2 \qquad \text{(B.6.1.3)}$$

From (B.6.1.3) the parameters of such transformations should satisfy the following three relations:

$$\begin{aligned} &|a_{11}|^2 + |a_{12}|^2 = 1, \\ &|a_{21}|^2 + |a_{22}|^2 = 1, \\ &a_{11}a_{12} + a_{21}a_{22} = 0. \end{aligned} \qquad \text{(B.6.1.4)}$$

All such transformations form an orthogonal group in two dimensions O(2).

An equivalent definition: O(2) is a group formed by all real orthogonal (2×2) matrices.

B.6.2 O(n)

All real orthogonal $(n \times n)$ matrices form the n (n-1)/2 - parameter *real orthogonal group* O(n).

The group O(n) is a subgroup of the group GL(n).

B.6.3 SO(n)

All real orthogonal $(n \times n)$ matrices whose determinants are equal to +1 form the *special orthogonal group* SO(n).

The group SO(n) is a subgroup of the group O(n).

B.6.4 SO(1,1)

Let us consider the linear transformations in two dimensions [69]:

$$\begin{aligned} x' &= a_{11}x + a_{12}y \\ y' &= a_{21}x + a_{22}y \end{aligned} \qquad \text{(B.6.4.1)}$$

where the parameters a_{11}, a_{12}, a_{21} and a_{22} as well as the coordinates x and y take only real values,

$$\begin{vmatrix} a_{11} & a_{12} \\ a_{21} & a_{22} \end{vmatrix} = 1 \qquad \text{(B.6.4.2)}$$

and which preserve the relation:

$$x'^2 - y'^2 = x^2 - y^2 .$$

All such transformations form a group in two dimensions SO(1,1).

B.6.5 SO(p,q)

All real $((p + q) \times (p + q))$ matrices whose determinants are equal to +1 and which keep invariant the quadratic form

$$x_1^2 + x_2^2 + \ldots + x_p^2 + x_{p+1}^2 + x_{p+q}^2 = inv \qquad \text{(B.6.5.1)}$$

comprise a group SO(p,q).

B.7 Symplectic group

Let us consider the linear transformations of two points in a plane (x_1, y_1), and (x_2, y_2) [69]:

$$\begin{aligned} x_1' &= a_{11}x_1 + a_{12}y_1 \\ y_1' &= a_{21}x_1 + a_{22}y_1 \end{aligned} \qquad \text{(B.7.1)}$$

and

$$\begin{aligned} x_2' &= a_{11}x_2 + a_{12}y_2 \\ y_2' &= a_{21}x_2 + a_{22}y_2 \end{aligned} \qquad \text{(B.7.2)}$$

and let us require that the following relation holds:

$$x_1'y_2' - y_1'x_2' = x_1y_2 - y_1x_2 . \qquad \text{(B.7.3)}$$

All such transformations form a group in two dimensions called the *symplectic group*. If the parameters a_{11}, a_{12}, a_{21} and a_{22} are complex then the group is denoted as Sp(4, C). If the parameters a_{11}, a_{12}, a_{21} and a_{22} are real then the group is denoted as Sp(4,R). If we require that the transformations of Sp(4,C) be unitary, then we will get the unitary symplectic group denoted as Sp(4).

This can be generalized for n dimensions. Then the corresponding groups will be Sp(2n,C), Sp(2n,R) and Sp(2n).

References

[1] P. Van Isacker, "*Symmetries in N~Z Nuclei*", GANIL, France, (http://www.ganil.fr/research/nt/symmetry1). (Private communication)

[2] P. Van Isacker, "*The Interacting Boson Model*", GANIL, France, (http://www.ganil.fr/research/nt/symmetry2).

[3] D. J. Rowe, C. Bahri, and W. Wijesundera, Phys. Rev. Lett. **80**, 4394, (1998).

[4] F. Iachello, N.V. Zamfir, and R.F. Casten, Phys. Rev. Lett. **81**, 1191, (1998).

[5] R.F. Casten, D. Kusnezov, and N.V. Zamfir, Phys. Rev. Lett. **82**, 5000, (1999).

[6] J. Jolie, P. Cejnar, and J. Dobeš, Phys. Rev. C **60**, 061303, (1999).

[7] F. Iachello, Phys. Rev. Lett. **85**, 3580, (2000). (Private communication)

[8] F. Iachello, Phys. Rev. Lett. **87**, 052502, (2001).

[9] F. Iachello and A. Arima, "*The Interacting Boson Model*". Cambridge University Press, Cambridge, (1987).

[10] J. Jolie, R.F. Casten, P. von Brentano and V. Werner, Phys. Rev. Lett. **87**, 162501, (2001).

[11] D. D. Warner, "*IBM symmetries and phases*", Nature, **420**, 614, (2000).

[12] O. Castaños, P. Federman, A. Frank, and S. Pittel, Nucl. Phys. A **379**, 61, (1982).

[13] A. Frank, Phys. Rev. C **39**, 652, (1989).

[14] A. Gómez, O. Castaños, and A. Frank, Nucl. Phys. A **589**, 267, (1995).

[15] D.D. Warner and R.F. Casten, Phys. Rev. Lett. **48**, 1385, (1982).

[16] R.F. Casten and N.V. Zamfir, Phys. Rev. Lett. **85**, 3584 (2000).

[17] R. Krücken et al, Phys. Rev. Lett. **88**, 232501, (2002).

[18] J. Escher and A. Leviatan, Phys. Rev. Lett. **84**, 1866 (2000).

[19] D. Bonatsos, D. Lenis, N. Minkov, P. P. Raychev and P. A. Terziev, Phys. Rev. Lett. **86**, 2052 (2001).

[20] V. Werner, N. Pietralla, P. von Brentano, R.F. Casten and R.V. Jolos, "*Quadrupole shape invariants in the interacting boson model* ", (http://arXiv: nucl-th/0005013 v1, 6 May 2000).

[21] J. N. Ginocchio, and A. Leviatan, "*Critical points in nuclei and interacting boson model intrinsic states*", (http://arXiv: nucl-th/0305013 v1, 6 May 2003).

[22] J. M. Arias, C. E. Alonso, A. Vitturi, J. E. García-Ramos, J. Dukelsky and A. Frank, "*The U(5)–O(6) transition in the Interacting Boson Model and the E*(5) *critical point symmetry* ", (http://arXiv: nucl-th/0309005 v1, 2 Sep. 2003).

[23] J. Dukelsky, J. M. Arias, J. E. García-Ramos and S. Pittel, "*Integrability and quantum phase transitions in interacting boson models* ", (http://arXiv: nucl-th/ th/0310031 v1, 9 Oct. 2003).

[24] J. P. Draayer, V. G. Gueorguiev, Feng Pan, and Yanan Luo, "*Mixed symmetry nuclear shell model*", (http://arXiv: nucl-th/0311094 v1, 26 Nov. 2003).

[25] V. Werner, P. von Brentano, R. F. Casten and J. Jolie, "*Singular character of critical points in nuclei*", (http://arXiv: nucl-th/0106051 v2, 12 Dec. 2001).

[26] E. A. McCutchan, N. V. Zamfir, M. A. Caprio, R. F. Casten, H. Amro, C. W. Beausang, D. S. Brenner, A. A. Hecht, C. Hutter, S. D. Langdown, D. A. Meyer, P. H. Regan, J. J. Ressler and A.D. Yamamoto, Phys. Rev. C**69,** 024308 (2004).

[27] R. Bijker, R. F. Casten, N. V. Zamfir and E. A. McCutchan, "*A Test of X(5) for the γ-degree of freedom* ", (http://arXiv: nucl-th/0311032 v1, 10 Nov. 2003).

[28] Z. Jin-Fu, L. Gui-Lu, S. Yang, Z. Sheng-Jiang, L. Feng-Ying and Jia Ying, *Chinese Phys. Lett.* **20**, 1231-1233 (2003).

[29] Z. Da-Li and L. Yu-Xin, *Chinese Phys. Lett.* **20**, 1028-1030 (2003)

[30] V. N. Zamfir and R. F. Casten, *Proceedings Of The Romanian Academy*, *Series A*, Vol. 4, No. 2, (2003).

[31] D. Tonev, "*Transition probabilities in ^{154}Gd-test for Critical Point Symmetry X(5)* ",(http://arXiv: nucl-th/0402087 v1, 25 Feb. 2004).

[32] E. López-Moreno and O. Castaños, Phys. Rev. C **54**, 2374, (1996).

[33] E. López-Moreno, PhD thesis, Universidad Nacional Autónoma de México, (1998).

[34] R. Gilmore. "*Catastrophe theory for scientists and engineers*". Wiley, New York, (1981).

[35] D. Janssen, R. V. Jolos, and F. Dönau, Nucl. Phys. A **224**,93, (1974).

[36] A. Arima, and F. Iachello, Phys. Rev. Lett. **35**, 1069, (1975).

[37] A. Arima, and F. Iachello, Phys. Rev. C**16**, 2085, (1977).

[38] A. DeShalit and I. Talmi, "*Nuclear shell theory*", Academic press, New York, (1963).

[39] D. Bonatsos, "*Interacting boson models of nuclear structure*", Clarendon Press, Oxford, (1988).

[40] R. Fossion, C. De Coster, J.E. García-Ramos, T. Werner, and K. Heyde, Nucl. Phys. A **697**,703, (2002).

[41] G. Audi and A.H. Wapstra, Nucl. Phys. A **595**, 409, (1995).

[42] W.T. Chou, N.V. Zamfir, and R.F. Casten, Phys. Rev. C **56**, 829, (1997).

[43] O. Scholten, "*Computer Program PHINT* ", Groningen Univ., The Netherlands, (1979).

[44] O. Scholten, "*The shortened version of PHINT* ", Published in Computational Nuclear Physics 1, p.88, (1991). (http://www.phys.washington.edu/users/bulgac/Koonin/IBA/pcibaxw.for)

[45] O. Scholten, "*The shortened version of PBEM* ", Published in Computational Nuclear Physics 1, p.88, (1991) (http://www.phys.washington.edu/users/bulgac/Koonin/IBA/pcibaem.for)

[46] A.A. Sonzogni, Nucl. Data Sheets **93**, 599, (2001).

[47] L.K. Peker and J.K. Tuli, Nucl. Data Sheets **82**, 187, (1997).

[48] M.R. Bhat, Nucl. Data Sheets **89**, 797, (2000).

[49] E. Dermateosian and J.K Tuli, Nucl. Data Sheets **75**, 827, (1995).

[50] Agda Artna-Cohen, Nucl. Data Sheets **79**, 1, (1996).

[51] C.W. Reich and R.G. Helmer, Nucl. Data Sheets **85**, 171, (1998).

[52] R.G. Helmer, Nucl. Data Sheets **65**, 65, (1992).

[53] R.G. Helmer, Nucl. Data Sheets **77**, 471, (1996).

[54] C.W. Reich, Nucl. Data Sheets **78**, 547, (1996).

[55] R.G. Helmer and C.W. Reich, Nucl. Data Sheets **87**, 317, (1999).

[56] Balraj Singh, Nucl. Data Sheets **93**, 243, (2001).

[57] E.N. Shurshikov and N.V. Timofeeva, Nucl. Data Sheets **67**, 45, (1992).

[58] P. J. Brussaard and P. W. M. Glaudemans, "*Shell-Model Applications in Nuclear Spectroscopy*", North Holland Publishing Company, North Holland, (1977).

[59] J.N. Ginocchio and M.W. Kirson, Nucl. Phys. A **350**, 31, (1980).

[60] A. E. L. Dieperink and O. Scholten, Nucl. Phys. A **346**, 125, (1980).

[61] A.E.L. Dieperink, O. Scholten, and F. Iachello, Phys. Rev. Lett. **44**, 1747, (1980).

[62] P. Cejnar and J. Jolie, Phys. Rev. E 61, 6237, (2000).

[63] J. Dukelsky, G.G. Dussel, R.P.J. Perazzo, S.L. Reich, and H.M. Sofia, Nucl. Phys. A **425**, 93, (1984).

[64] P. Van Isacker and J.Q. Chen, Phys. Rev. C **24** 684, (1981).

[65] H.E. Standley, "*Introduction to phase transitions and critical phenomena*", Oxford University Press, Oxford (1971).

[66] R.F. Casten and N.V. Zamfir, Phys. Rev. Lett. **87**, 052503, (2001).

[67] E. Wigner, "*Group Theory and its Application to the Quantum Mechanics of Atomic Spectra*", Academic Press, New York, (1959).

[68] M. Hamermesh, "*Group Theory and its Application to Physical Problems*", Addison-Wesley Reading, MA, (1962).

[69] J. P. Elliott and P.G. Dawber, "*Symmetry in Physics*", The Macmillan Press, London, (1979).

دراسة التحولات الطوريه والنقاط الحرجة في منطقة العناصر الأرضية النادرة ضمن إطار نموذج البوزونات المتفاعلة (IBM-1)

رسالة مقدمّة إلى

مجلس كلية العلوم - جامعة النهرين

وهي جزء من متطلبات نيل درجة دكتوراه فلسفة في الفيزياء

من قبل

فؤاد عطية مجيد العجيلي

(بكالوريوس ١٩٩٧)

(ماجستير ١٩٩٩)

صُفر ١٤٢٦هـ

نيسان ٢٠٠٥ م

الخلاصة

أجريت دراسة تصنيفيه لسلسله من النظائر في منطقة العناصر الأرضية النادرة، حيث تمت عملية وصف لمستويات الطاقة ومعدلات الانتقال E2 وطاقات الفصل بين نيوترونين للسلاسل $^{144-154}_{60}Nd$ ، $^{146-160}_{62}Sm$ ، $^{148-162}_{64}Gd$ و $^{150-166}_{66}Dy$ باستخدام الشكل العام للهاملتونين الخاص بنموذج البوزونات المتفاعلة (IBM-1).

تم أجراء ملائمة شمولية (General fit) لكل سلسله من النظائر، بحيث تكون كل الثوابت المُحددة في داله الهاملتونين ثابتة ما عدا واحد متغيّر لوصف السلسلة بكاملها.

في منطقة العناصر الأرضية النادرة تتحول النويات من الأشكال الكروية إلى الأشكال المشوهة، وبالأعتماد على النظرية المسماة بـ (Catastrophe theory) عن طريق ربطها مع تحليلات الحالة المتشاكهة (Coherent state analysis) تم توليد أسطح الطاقة لنموذج البوزونات المتفاعلة (IBM-1) وبالتالي تعيين النويات التي تكون قريبة من نقاط التحول الطوري الحرجة.

أن الطريقة التي تم أتباعها لحساب الثوابت المُحددة للهاملتونين قادت بشكل عام إلى نتائج جيده جداً مقارنةً مع النتائج العملية المتوفرة حديثاً لكل من طاقات التهيج ومعدلات الأنتقال E2 وطاقات الفصل بين نيوترونين S_{2n}. من الجدير بالذكر هنا وبشكل خاص أنه تم الحصول على نتائج تتفق بشكل ممتاز عند مقارنة النتائج النظرية مع النتائج العملية

لطاقات الفصل بين نيوترونين S_{2n} والتي يمكن أعتبارها كمؤشر جدير بالملاحظة لتحديد مناطق التحول الطوري.

أن التحليلات المُتّبعة في هذا العمل أعطت نتائج متناغمة مع الدراسات السابقة التي أستخدم فيها هاملتونين (CQF) لنفس المنطقه. وكمحصلة لهذا العمل وجدنا أن ^{148}Nd و ^{150}Sm يعتبران المرشحين الأفضل ليكونا في النقطة الحرجة، ولكن مما تجدر الإشارة أليه أن ^{150}Nd و ^{152}Sm لا يبتعدان كثيرا عن النقطة الحرجة.